Available online at www.sciencedirect.com
ScienceDirect
International Journal of Approximate Reasoning
48 (2008) 437–465
INTERNATIONAL JOURNAL OF APPROXIMATE REASONING
www.elsevier.com/locate/ijar

Defining belief functions using mathematical morphology – Application to image fusion under imprecision

Isabelle Bloch

Ecole Nationale Supérieure des Télécommunications (GET – Télécom Paris), CNRS UMR 5141 LTCI – Signal and Image Processing Department, 46 rue Barrault, 75013 Paris, France

Received 21 August 2006; received in revised form 12 July 2007; accepted 13 July 2007
Available online 11 August 2007

Abstract

We address in this paper the problem of defining belief functions, typically for multi-source classification applications in image processing. We propose to use mathematical morphology for introducing imprecision in the mass and belief functions while estimating disjunctions of hypotheses. The basic idea relies on the similarity between some properties of morphological operators and properties of belief functions. The framework of mathematical morphology guarantees that the derived functions have all required properties. We illustrate the proposed approach on synthetic and real images.

Keywords: Mathematical morphology; Dilation; Erosion; Belief functions; Dempster–Shafer theory; Image fusion; Spatial imprecision; Fuzzy sets

1. Introduction

Information fusion in image processing has led to an increased interest during the last years, motivated by the development of multiple acquisition techniques. These techniques are more and more jointly used to give access to a better knowledge in many cases of experimental sciences. In image processing, information fusion appears as a necessary stage for applications like medical imaging, aerial and satellite imaging, quality control, robot vision, vehicle or robot guidance. It allows solving problems that could not be solved by using only one type of acquisition, due to its imperfections and incompleteness.

A main issue in this domain is to represent the different types of imperfections (imprecision, uncertainty, ambiguity, incompleteness, unreliability, conflict, etc.) and to cope with them. Numerous approaches have been developed in order to answer the difficult question of image fusion in different application domains [1]. Among them, numerical methods (either based on probabilistic models or on non-probabilistic ones) have gained a large interest because of their ability (i) to model image information, the specificities of the information provided by each image for each hypothesis, along with its imperfections, and (ii) to reason under different types of imperfections. In particular, methods based on belief functions [2,3] have led to interesting

E-mail address: Isabelle.Bloch@enst.fr

0888-613X/$ - see front matter
doi:10.1016/j.ijar.2007.07.008

developments and promising results in the recent years. The typical scheme consists in (i) defining a set of discernment that represents the hypotheses of interest for the decision making step (typically classes in a multi-source classification problem), (ii) estimating mass functions from characteristics of the classes in each image, (iii) combining the mass functions of all images, (iv) making decision based on computation of belief, plausibility or pignistic probability functions.

One of the difficulties when using belief functions theory for image fusion consists in estimating mass functions on disjunctions, to provide a proper representation of imprecision in the information provided by each image. This can be imprecision in grey levels characterizing the classes of interest in each image, or imprecision in the spatial domain (due for instance to preliminary registration between the images, poor object delineation, partial volume effect, noise, etc.). Examples where it is very useful to take disjunctions into account in the modeling step, and where belief functions theory provides appropriate answers, include the following situations:

- a source provides information concerning only a few of several classes;
- a source does not differentiate two classes: hesitation or ambiguity between these two classes is then modeled as a mass on the disjunction of these two classes;
- partial volume effect or mixed pixels due to the discrete nature of the images (a situation that often occurs at the border of classes): it can also be taken into account by assigning masses to the union of the two classes mixed in the considered area;
- a global source reliability has to be taken into account: this may be done by weakening all masses and reinforcing $m(D)$, D being the set of discernment, hence the largest disjunction, using a discounting process;
- knowledge of source reliability is available only for some classes: it can be taken into account by modifying accordingly the masses assigned to these classes and in order to take ignorance into account without forcing values for something unknown.

Let us illustrate some of these issues on two simple examples. In the first example in Fig. 1, the two images represent degraded observations of a two-class image (a white square on a black background). Due to the noise, making a decision about the membership of a point to one of the classes based only on the grey levels of this

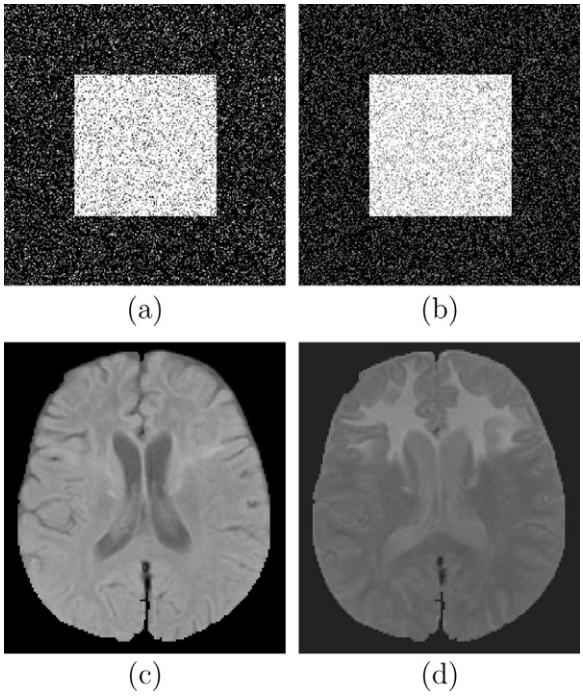

Fig. 1. (a,b) Two noisy observations of a two-classes image. (c,d) One axial slice of dual-echo magnetic resonance imaging acquisitions (pathological brain image) – Courtesy Professor Catherine Adamsbaum, Saint Vincent de Paul Hospital, Paris.

point in the two observations would lead to a very noisy result. This can be corrected by introducing imprecision at the modeling level, so as to guarantee a better spatial consistency in the final result. The second example in Fig. 1 concerns real images from the medical imaging domain. Here, due to the limited resolution, a partial volume effect results in intermediate grey levels at points composed of a mixture of several ''pure'' classes (typically at the boundary of these classes). This can be modeled using disjunctions of these classes, for instance by defining mass functions on a grey level space. Another issue in this example is that a pathology (bright area) is visible in the second image but not in the first one. Again this can be modeled using a disjunction of the classes that are seen with similar grey levels in one image. These two examples will be further detailed in this paper.

Let us summarize the main existing approaches for defining mass functions. It should be noted that it remains a partially unsolved problem, which did not yet find a general answer. The difficulty is even increased if masses have to be assigned to disjunctions [4,5]. In image processing, they may be derived at three different levels. At the highest, most abstract and symbolic level, information representation is used in a way similar to that in artificial intelligence and masses are assigned to propositions, often provided by experts [6–8]. Up to now, this kind of information is usually not derived from measures on the images. At an intermediate level, masses are computed from attributes, and may involve simple geometrical models [9–12]. This is well adapted to model-based pattern recognition but it is difficult to use for image fusion classification of complex structures without a model. At the pixel level, several methods can be applied for mass assignment, and most of them are inspired by statistical pattern recognition. The easiest way consists in computing masses on singletons in each source often based on a probabilistic estimation. Masses on all other subsets of the frame of discernment D are then zero. This model is very restricted and does not exploit the interesting features of belief function theory. However, a lot of approaches are based on this initial model and then assign masses on disjunctions (or on some of them) in a simple and often quite heuristic way [10,13–15]. Recent work addressed the problem of estimating belief functions from sample data. For instance, in [16], belief functions are estimated from realizations of a random variable, with the constraint that they converge towards the probability distribution of this variable when the sample size goes towards infinity.

Let us mention a few other possible models, which include disjunctions:

Modification of probabilistic models. The easiest and most used model consists in using a discounting procedure [3]. In the case where initial masses are learned on singletons only, for instance from probabilities, then a mass on D is directly derived from the discounting factor. This technique is often used in order to weaken a source depending on its reliability, and allows assigning a mass to D which will be low if the source is reliable, and high if it is not. This type of model is very simple. Learning masses on singletons can benefit from classical statistical learning techniques. However, disjunctions other than D are not modeled, which strongly limits the power of this model.

Two probability-inspired models have been proposed in [17], and take into account other disjunctions than D. These models assume an initial estimation of conditional probabilities. The associated mass function is computed by combining mass functions associated to each singleton, using discounting and source reliability factors. This model is well adapted in cases where we can learn a class against all the others, as is often the case in pattern recognition in images, or in cases where each class is determined from an adapted detector (for instance a road detector in an aerial image allows us to define the probability of belonging to the road against all the other classes, but is not able to distinguish between these other classes).

In [18], disjunctions are defined as a function of a significance criterion of conditional probabilities. If several probability values are significant, then the corresponding disjunctions are taken into account, based on differences between the probability values.

Modification of distance models. A pattern recognition like approach is proposed in [19]. If each class or hypothesis is represented by a prototype (or a center), a mass function associated to each class can be defined, for which this class and D are the only focal elements, based on a function of the distance of each element to the prototype. The masses are then combined using Dempster's rule in order to get a mass which takes into account the information on all classes. This approach can also be applied to the k nearest neighbors.

A priori on the disjunctions. In several applications, some *a priori* may be available and allows determining in a supervised way which are the focal elements that should be considered. These methods are used for instance in [20–22]. In [20], brain images are combined in order to detect pathologies. The mass functions are determined in an automatic way from grey levels [23] and classes that are not distinguished in some images

are grouped into disjunctions. In [22], results obtained from several detectors (for several types of structures) are combined in order to interpret a radar image. The focal elements are determined from the capabilities of detectors to differentiate or not several classes. In [21], attributes extracted from images from different sensors are combined in order to differentiate mines from non-dangerous objects, in the context of humanitarian demining. The measures to be combined can characterize either a class or the whole set of discernment.

This type of approach is very efficient if such information is available, but it remains supervised, and therefore is applicable only to problems for which the cardinality of D has a reasonably low value.

Learning the disjunctions. Methods for learning focal elements are often based on preliminary classifications performed on each source separately. For instance, from confusion matrices it is possible to identify classes which are often mixed up in a source, and the union of such classes then constitutes a focal element of the mass function attached to this source [24].

In a completely unsupervised way, intersections between classes detected in a source and classes detected in another one can be used to define singletons of the space of discernment. The classes detected in each source are then expressed as disjunctions of these singletons [25].

Measures of dissonance and consonance have been proposed in [26]. The idea consists in modifying an initial mass function on singletons by discounting the mass values according to the consonance between singletons, and by assigning masses on disjunctions of two classes according to the degree of dissonance between these classes. This method has been applied to the fusion of several classifiers. The consonance of a class is computed from the number of elements assigned to this class by all classifiers, and the dissonance from the number of elements classified differently.

In the case where elements are characterized by a measurement in a one-dimensional space (typically represented as an histogram), masses on compound hypotheses can be defined in overlap or ambiguity areas between two neighbor classes.

Another method, inspired by hierarchical thresholding methods, is proposed in [27]: each histogram peak corresponds to a singleton. Then the histogram is progressively thresholded at decreasing heights, and disjunctions are created when maxima are merged. This method is similar to component tree used for instance in mathematical morphology [28]. It is also close to the confidence intervals and their links with possibility distributions [29].

In this paper, we show that fuzzy mathematical morphology [30] provides useful tools for introducing imprecision in the mass functions while estimating compound hypotheses (disjunctions), in an original way. It extends and develops the ideas presented earlier in [31]. The underlying assumption is that it is possible to represent imprecision by a set or a fuzzy set, called structuring element. The proposed method consists then of a rigorous approach to introduce this imprecision in belief function models. This approach can be applied in a characteristics space, to account for imprecision on these characteristics (such as grey levels for instance) or in the spatial domain, to account for spatial information.

Another approach for introducing spatial information in belief functions consists in merging them with a Markov random field, as proposed in [32,33]. This approach relies on a probabilistic semantics and leads to a result which is also a Markov field. Our approach differs on these two points: the semantics is not necessarily of probabilistic nature and disjunctions are taken into account until the last step.

In Section 2, we briefly summarize the basic concepts of mathematical morphology and belief functions that are involved in the proposed method. In Section 3, we propose the mathematical foundations of a new method for computing belief and plausibility functions using morphological operators in the case of two focal elements. In Section 4, we extend this method to more than two hypotheses. In Section 5, we propose several schemes for applying this method to image fusion problems, and provide illustrating examples on synthetic and real images.

2. Mathematical morphology, belief functions and fuzzy sets

2.1. Background notions in mathematical morphology

Mathematical morphology [34–37] operators are defined on complete lattices, i.e. partially ordered sets $(\mathcal{T}, \leqslant)$ in which every non-void part X has a supremum, denoted by $\vee X$, and an infimum, denoted by $\wedge X$.

Typically $\mathcal{T}$ can be the power set of a set E, $\leqslant$ being the inclusion, or the lattice of functions, such as grey level functions defining images, $\leqslant$ being the classical partial order on numerical functions. The two main operations are dilation δ and erosion ε, defined as operators from $\mathcal{T}$ into $\mathcal{T}$ that commute with the supremum and the infimum, respectively.

In image processing, sets and functions are defined on a underlying spatial domain (an affine space), denoted by $\mathcal{S}$ (typically $\mathbb{R}^n$ or $\mathbb{Z}^n$ in the digital case), and $\mathcal{T}$ is the lattice of subsets of $\mathcal{S}$ or the lattice of functions on $\mathcal{S}$. The underlying space $\mathcal{S}$ can also represent a feature space, such as the grey level axis for instance. Particular types of dilations and erosions, widely used in image processing, are invariant by translation (in $\mathcal{S}$) and can be expressed via the definition of a structuring element. On the lattice of sets, for a structuring element B (a subset of $\mathcal{S}$), the morphological dilation of a set $X \subseteq \mathcal{S}$ is defined as

$$\delta_B(X) = \{x \in X, \check{B}_x \cap X \neq \emptyset\}, \tag{1}$$

where $\check{B}_x$ denotes the symmetrical of the structuring element translated at x (in the following, we consider only structuring elements which are symmetrical with respect to the origin, i.e. $B = \check{B}$). The morphological erosion of X is defined as

$$\varepsilon_B(X) = \{x \in X, B_x \subseteq X\}. \tag{2}$$

On the lattice of numerical functions defined on $\mathcal{S}$, dilation and erosion by a flat structuring element B (i.e. a subset of $\mathcal{S}$) are expressed by

$$\delta_B(f)(x) = \sup_{y \in B_x} f(y), \tag{3}$$

$$\varepsilon_B(f)(x) = \inf_{y \in B_x} f(y). \tag{4}$$

In these equations, x denotes a point of $\mathcal{S}$. The functions are defined on $\mathcal{S}$ and take numerical values.

From dilation and erosion, two other operators are defined by composition: morphological opening ($\gamma = \delta\varepsilon$, i.e. $\forall a \in \mathcal{T}, \gamma(a) = \delta(\varepsilon(a))$) and closing ($\varphi = \varepsilon\delta$).

Let us summarize the main properties of these operations. For general algebraic dilations and erosions, the following properties hold:

- By definition, ε commutes with the conjunction and δ with the disjunction:

$$\forall (a_i, i \in I) \subseteq \mathcal{T}, \quad \varepsilon\left(\bigwedge_{i \in I} a_i\right) = \bigwedge_{i \in I} \varepsilon(a_i),$$

$$\forall (a_i, i \in I) \subseteq \mathcal{T}, \quad \delta\left(\bigvee_{i \in I} a_i\right) = \bigvee_{i \in I} \delta(a_i).$$

- The pair (ε, δ) forms an adjunction:

$$\forall a \in \mathcal{T},\ \forall b \in \mathcal{T}, \quad \delta(a) \leqslant b \Longleftrightarrow a \leqslant \varepsilon(b).$$

- ε and δ are increasing with respect to $\leqslant$.
- We have

$$\varepsilon\delta\varepsilon = \varepsilon \quad \text{and} \quad \delta\varepsilon\delta = \delta$$

hence the idempotence of $\delta\varepsilon$ (morphological opening, denoted by γ) and $\varepsilon\delta$ (morphological closing, denoted by φ).

- Opening is anti-extensive and closing is extensive

$$\delta\varepsilon \leqslant Id \quad \text{and} \quad \varepsilon\delta \geqslant Id,$$

where Id denotes the identity operator on $\mathcal{T}$, mapping every element on itself (i.e. $\forall a \in \mathcal{T}, Id(a) = a$).

Some additional properties hold in the specific case of morphological operations, assuming an underlying affine space $\mathcal{S}$ and a structuring element B:

- Morphological dilation and erosion (using a structuring element) are dual operators with respect to the complementation. Similarly, opening and closing are dual operators. For instance if $\mathscr{T}$ is the lattice of sets and B is a symmetrical structuring element, then we have

$$\delta_B(X) = \overline{\varepsilon_B(\overline{X})} \tag{5}$$

where $\overline{X}$ denotes the complement of X in the underlying space. Similarly, if $\mathscr{T}$ is the lattice of functions of $\mathscr{S}$ into $[0,1]$, duality is expressed by

$$\forall x \in \mathscr{S}, \quad \delta_B(f)(x) = 1 - \varepsilon_B(1-f)(x). \tag{6}$$

Similar relationships hold between opening and closing.

- For definitions based on a structuring element, if the origin belongs to the structuring element ($O \in B$), then ε_B is anti-extensive and δ_B is extensive, i.e.

$$\varepsilon_B \leqslant Id \quad \text{and} \quad \delta_B \geqslant Id.$$

2.2. Links with properties of belief functions

Formally, the required properties for defining or characterizing belief (*Bel*) and plausibility (*Pls*) functions defined on a set of discernment D are the following [3,2,38]:

$$Bel(\emptyset) = Pls(\emptyset) = 0, \quad Bel(D) = Pls(D) = 1, \tag{7}$$

$$\forall A_1, \ldots A_n (A_i \subseteq D), \quad Bel(\cup_{i=1\ldots n} A_i) \geqslant \sum_{I \subseteq \{1\ldots n\}, I \neq \emptyset} (-1)^{|I|+1} Bel(\cap_{i \in I} A_i), \tag{8}$$

$$\forall A \subseteq D, \quad Bel(A) = \sum_{B \subseteq A, B \neq \emptyset} m(B), \tag{9}$$

$$\forall A \subseteq D, \quad Pls(A) = 1 - Bel(\overline{A}), \tag{10}$$

$$\forall A \subseteq D, \quad Bel(A) \leqslant Pls(A). \tag{11}$$

Given a normalized mass function, i.e. a function from 2^D into $[0,1]$ such that $\sum_{A \subseteq D} m(A) = 1$ and $m(\emptyset) = 0$, a belief function can be derived using Eq. (9) and then satisfies properties expressed in Eqs. (7) and (8). Conversely, there exists a mass function satisfying Eq. (9) for any belief function defined by Eqs. (7) and (8). An axiomatic justification of the use of belief functions as an appropriate modeling of quantified beliefs can be found in [38].

These formulas assume an underlying closed-world assumption, in which $m(\emptyset) = 0$. If this constraint is relaxed (open-world assumption), then some of the formulas are slightly modified: $Bel(D) = 1 - m(\emptyset)$ and $Pls(A) = Bel(D) - Bel(\overline{A})$.

When several sources have to be combined in a conjunctive way, the resulting mass function m is obtained from the masses of each source m_i using Dempster's rule [3,2], expressed in its unnormalized form as

$$m(A) = (m_1 \oplus m_2 \oplus \cdots \oplus m_n)(A) = \sum_{B_1 \cap \cdots \cap B_n = A} m_1(B_1) m_2(B_2) \cdots m_n(B_n),$$

which may lead to a non-zero mass on the empty set.

The main idea of this paper is to exploit the similarities between some properties of mathematical morphology and of belief functions. In particular, duality holds in both theories between some pairs of operators and functions (Eqs. (5) and (6) on the one hand, and Eq. (10) on the other hand). Also anti-extensivity of erosion and extensivity of dilation (when they hold, i.e. when $O \in B$) lead to

$$\varepsilon_B \leqslant \delta_B, \tag{12}$$

which is similar to Eq. (11) between belief and plausibility functions. Similar resemblances exist when using opening ($\gamma_B = \delta_B \varepsilon_B$) and closing ($\varphi_B = \varepsilon_B \delta_B$). Note that we always have $\gamma_B \leqslant \varphi_B$, whatever the choice of the structuring element B.

2.3. Fuzzy mathematical morphology

Let us now summarize extensions of mathematical morphology to fuzzy sets. They are in particular interesting for dealing with functions taking values into $[0,1]$ using operators based on non-flat structuring elements, i.e. which are themselves functions into $[0,1]$. Another advantage is for representing different types of imprecision. Although interpretations of membership functions, possibility distributions and mass or belief functions are undoubtedly quite different (but links exist, see e.g. [3,39–42]), two aspects are interesting for the proposed approach:

- formally we can use membership functions or possibility distributions for estimating mass functions using fuzzy mathematical morphology, since one of the strongest constraints in this theory is to deal with functions taking values in $[0,1]$ with operations that are internal in $[0,1]$; we defined mathematical morphology on fuzzy sets [30] based on membership functions, but the formal derivations apply to mass functions as well;
- fuzzy notions are very useful for introducing imprecision on the objects or classes in images, either on their characteristics (such as grey levels) or on their spatial extent.

Several definitions have been recently proposed for fuzzy morphology, e.g. [30,43–48]. A general principle for defining fuzzy mathematical morphology relies on the translation of set equations defining morphological operations on binary sets into their functional (or fuzzy) equivalents [30]. This leads to the following definitions for the dilation $\delta_v(\mu)$ and erosion $\varepsilon_v(\mu)$ of a fuzzy set μ by a fuzzy structuring element v defined on a space $\mathscr{S}$ (typically $\mathbb{R}^n$):

$$\forall x \in \mathscr{S}, \quad \delta_v(\mu)(x) = \sup_{y \in \mathscr{S}} \top[\mu(y), v(x-y)], \tag{13}$$

$$\forall x \in \mathscr{S}, \quad \varepsilon_v(\mu)(x) = \inf_{y \in \mathscr{S}} \perp [\mu(y), c(v(y-x))], \tag{14}$$

where $\top$ is a t-norm and $\perp$ the t-conorm dual of $\top$ with respect to a complementation c (which automatically guarantees the duality between δ and ε). In the following, the following complementation is used:

$$\forall t \in [0,1], \quad c(t) = 1 - t. \tag{15}$$

Fuzzy opening and closing are then defined as the combination of an erosion followed by a dilation (resp. a dilation followed by an erosion) using the same structuring element, as in the classical case.

These definitions for the basic operators have excellent properties with respect to mathematical morphology and with respect to fuzzy sets [30]. At first, these operations are internal in $[0,1]$ (as opposed to the classical definitions on functions using functions as structuring elements [34]). Secondly, all properties of mathematical morphology are satisfied (for the basic operations and for the ones derived by combination like opening and closing), at least for particular t-norms and t-conorms. Most of them are satisfied whatever the choice of $\top$ and $\perp$. Here the condition for having anti-extensivity of ε and extensivity of δ is $v(O) = 1$, where O denotes the origin. This is equivalent to the condition $O \in B$ in the crisp case. Note that Eqs. (13) and (14) reduce to Eqs. (3) and (4) in the particular case where v is a crisp set (i.e. a flat structuring element), and to Eqs. (1) and (2) when both μ and v are crisp. Therefore, in the following we always denote the structuring element by v, for both the crisp and the fuzzy cases.

A second type of approach for fuzzy morphology is based on the notion of adjunction and fuzzy implications. Here the algebraic framework is the main guideline, which contrasts with the previous approach where duality was imposed in first place. The derivation of fuzzy morphological operators from residual implication has been proposed in [43], and then developed e.g. in [46,47]. This approach was formalized from the algebraic point of view of adjunction, as developed in [48]. The conditions under which the two approaches are equivalent have been proved in [49]. Here we use the first approach, since duality is a property of prime importance in order to derive belief and plausibility functions (Eq. (10)).

As a summary, the useful definitions for our purpose are the ones where operators are dual and applied with a structuring element such that $v(O) = 1$.

3. Belief functions from mathematical morphology in the case of two initial focal elements

In this section, we show how belief functions can be built from mathematical morphology operators in a consistent way. We first consider the case of two initial focal elements, which can be singletons of D or disjunctions of hypotheses.

With the aim of applying the following formalism to image fusion, we assume that all values of the functions (mass, belief, plausibility functions) are actually themselves functions defined over the considered space $\mathscr{S}$. This is perhaps a non-conventional way to deal with belief functions, but this can be interpreted in two ways. For each $x \in \mathscr{S}$, the set of values $m(A)(x)$, $Bel(A)(x)$, $Pls(A)(x)$ for all subsets A satisfy the properties of mass, belief and plausibility functions. Conversely, for each $A \subseteq D$, $m(A)$ is considered as a function from $\mathscr{S}$ to $[0,1]$ (which can be interpreted as a membership function or a possibility distribution for instance). As an example, Eq. (10) should be read $\forall A \subseteq D, \forall x \in \mathscr{S}, Pls(A)(x) = 1 - Bel(\overline{A})(x)$.

3.1. Construction

Fuzzy erosion and dilation (respectively opening and closing) are dual with respect to complementation, which suggests that they can be interpreted as belief and plausibility functions. Starting from an initial estimate of disjoint hypotheses (as usually obtained in image processing using probabilistic or fuzzy learning), it is possible to derive expressions for belief and plausibility by computing fuzzy erosion and dilation (or fuzzy opening and closing), from which new mass functions are deduced, both on singletons and on disjunctions of hypotheses, while taking into account the imprecision modeled as a structuring element.

Let us assume that we have an initial mass function m_0 defined over a frame of discernment D, and having only A and $\overline{A}$ as focal elements, with $A \subseteq D$ and $\overline{A} = D \setminus A$, such that

$$m_0(A) + m_0(\overline{A}) = 1. \tag{16}$$

In the case of $D = \{C_1, C_2\}$, we have $A = \{C_1\}$ and $\overline{A} = \{C_2\}$, but the assumption here is somewhat more general.

Imprecision on the definition of m_0 can be introduced through a structuring element v defined on $\mathscr{S}$ (it can be crisp or fuzzy), using mathematical morphology, by interpreting $m_0(A)$ and $m_0(\overline{A})$ as functions from $\mathscr{S}$ into $[0,1]$. We define belief and plausibility functions using two dual operators (typically erosion and dilation, or opening and closing). For erosion and dilation, we thus define:

$$Bel(A) = \varepsilon_v(m_0(A)), \quad Pls(A) = \delta_v(m_0(A)), \tag{17}$$

$$Bel(\overline{A}) = \varepsilon_v(m_0(\overline{A})), \quad Pls(\overline{A}) = \delta_v(m_0(\overline{A})). \tag{18}$$

Similarly, using opening and closing, we can define:

$$Bel(A) = \gamma_v(m_0(A)), \quad Pls(A) = \varphi_v(m_0(A)), \tag{19}$$

$$Bel(\overline{A}) = \gamma_v(m_0(\overline{A})), \quad Pls(\overline{A}) = \varphi_v(m_0(\overline{A})). \tag{20}$$

In the following, properties are derived for erosion and dilation, but they also hold for opening and closing. We always assume that the pairs of operators are chosen using dual definitions, and with $v(O) = 1$. This guarantees the properties of belief and plausibility functions.

3.2. Properties

Using the duality property between erosion and dilation, we have

$$\forall x \in \mathscr{S}, \quad Bel(\overline{A})(x) = \varepsilon_v(m_0(\overline{A}))(x) = \varepsilon_v(1 - m_0(A))(x) \tag{21}$$

$$= 1 - \delta_v(m_0(A))(x) = 1 - Pls(A)(x). \tag{22}$$

Similarly, we have $Bel(A)(x) = 1 - Pls(\overline{A})(x)$. Therefore, the expected duality between belief and plausibility holds (Eq. (10)). A similar result holds if we use opening and closing instead of erosion and dilation, or any other pair of dual operators.

Due to the property expressed by Eq. (12), we also have $Bel(A) \leqslant Pls(A)$, which is a required property of belief functions (Eq. (11)).

In order to prove that Eq. (8) holds, we just have to show in this case that $Bel(A) + Bel(\overline{A}) \leqslant 1$. This is straightforward, since we have

$$\begin{aligned} Bel(A) + Bel(\overline{A}) &= \varepsilon_v(m_0(A)) + 1 - \delta_v(m_0(A)) \\ &= 1 - [\delta_v(m_0(A)) - \varepsilon_v(m_0(A))]. \end{aligned}$$

Since both fuzzy erosion and dilation are internal into $[0,1]$, and due to property (12), we have $(Bel(A) + Bel(\overline{A})) \in [0, 1]$. This result also holds if we derive *Bel* and *Pls* from opening and closing.

If we set additionally $\forall x \in \mathscr{S}$, $Bel(\emptyset)(x) = Pls(\emptyset)(x) = 0$ and $Bel(D)(x) = Pls(D)(x) = 1$, we have all properties that should be satisfied by belief functions. They prove the consistency of our approach for defining belief and plausibility functions, according to the required properties as reviewed in Section 2.

The new mass function, derived according to Eq. (9), is easy to compute, $\forall x \in \mathscr{S}$:

$$\begin{aligned} &m(A)(x) = Bel(A)(x), \\ &m(\overline{A})(x) = Bel(\overline{A})(x) = 1 - Pls(A)(x), \\ &m(A \cup \overline{A})(x) = 1 - Bel(A)(x) - Bel(\overline{A})(x) \\ &\qquad = \delta_v(m_0(A))(x) - \varepsilon_v(m_0(A))(x) \\ &\qquad = \delta_v(m_0(\overline{A}))(x) - \varepsilon_v(m_0(\overline{A}))(x). \end{aligned} \tag{23}$$

This mass function includes the imprecision represented by v, and allows defining a mass value on the disjunction $A \cup \overline{A}$ (note that we have $0 \leqslant m(A \cup \overline{A}) \leqslant 1$ because of Eq. (12)). Note that this mass function corresponds exactly to the morphological gradient (difference between dilation and erosion), which is consistent with its interpretation in terms of transition between A and $\overline{A}$.

These results prove the following theorem.

Theorem 1. *Based on a normalized mass function with two focal elements A and $\overline{A}$, Eqs. (17) and (18) (respectively Eqs. (19) and (20)) provide belief, plausibility and mass functions that are consistent with belief function theory and that satisfy all required properties.*

Additional properties are directly derived from the properties of morphological operators (see Section 2). These properties (adjunction, etc.) are usually not considered in belief function theory, but it would be interesting to investigate to which extent they bring some new insights.

Interpretation of these formal derivations will be given in Section 3.4. As it appears from the above formulas, the proposed method is particularly suited for problems where we have to make a decision among two possible hypotheses (A or $\overline{A}$, A being either a singleton of D or a disjunction). In Sections 4 and 5, we will investigate how this approach can be used in a more general context.

3.3. Example

An example of such a construction where $\mathscr{S}$ is a 1D space is presented in Fig. 2. The initial mass function is defined on two disjoint hypotheses A_1 and A_2 such that $D = A_1 \cup A_2$. Each mass $m_0(A_i)$ is a function from $\mathscr{S}$ into $[0,1]$. At each point x of $\mathscr{S}$ we have $m_0(A_1)(x) + m_0(A_2)(x) = 1$. Erosion is performed using two different structuring elements, in order to illustrate the influence of its extension on the resulting belief functions and masses. For a structuring element v (chosen as a fuzzy structuring element having a paraboloid shape in this example), we have

$$\begin{aligned} &Bel(A_1)(x) = \varepsilon_v(m_0(A_1))(x) = \inf_{y \in \mathscr{S}} \perp (m_0(A_1)(y), 1 - v(y - x)), \\ &Bel(A_2)(x) = \varepsilon_v(m_0(A_2))(x) = \inf_{y \in \mathscr{S}} \perp (m_0(A_2)(y), 1 - v(y - x)), \\ &Pls(A_1)(x) = \delta_v(m_0(A_1))(x) = \sup_{y \in \mathscr{S}} \top (m_0(A_1)(y), v(x - y)), \\ &Pls(A_2)(x) = \delta_v(m_0(A_2))(x) = \sup_{y \in \mathscr{S}} \top (m_0(A_2)(y), v(x - y)). \end{aligned}$$

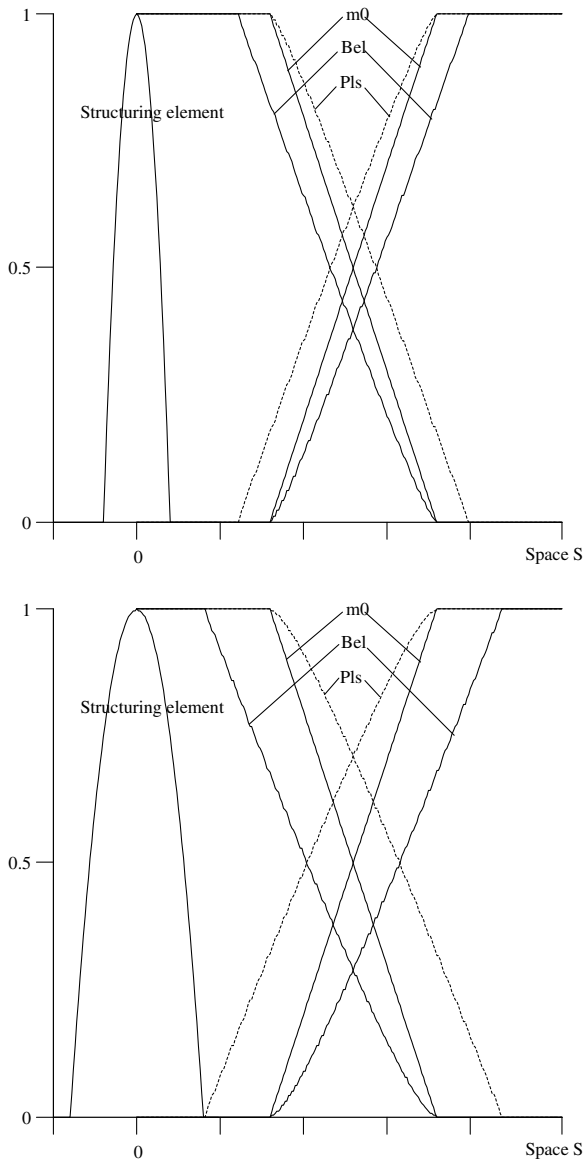

Fig. 2. Example of deriving belief and plausibility functions using fuzzy erosion (dotted lines) and dilation (dashed lines) using a paraboloid structuring element. The second example is obtained with a larger structuring element, leading to a larger effect on the transformed functions.

Due to the duality between $\perp$ and $\top$ with respect to the complementation and to the symmetry of ν with respect to the origin (i.e. $\nu(y-x)=\nu(x-y)$), we have

$$Pls(A_1)(x) = 1 - \inf_{y\in\mathscr{S}} \perp (1 - m_0(A_1)(y), 1 - \nu(y-x)) = 1 - Bel(A_2)(x),$$

$$Pls(A_2)(x) = 1 - Bel(A_1)(x).$$

Finally $m(D)$ is derived as $m(D)(x) = 1 - Bel(A_1)(x) - Bel(A_2)(x)$.

The resulting mass functions are shown in Fig. 3. Since the structuring element represents imprecision between the two hypotheses, it is consistent to observe that using a larger structuring element results in a larger mass on D.

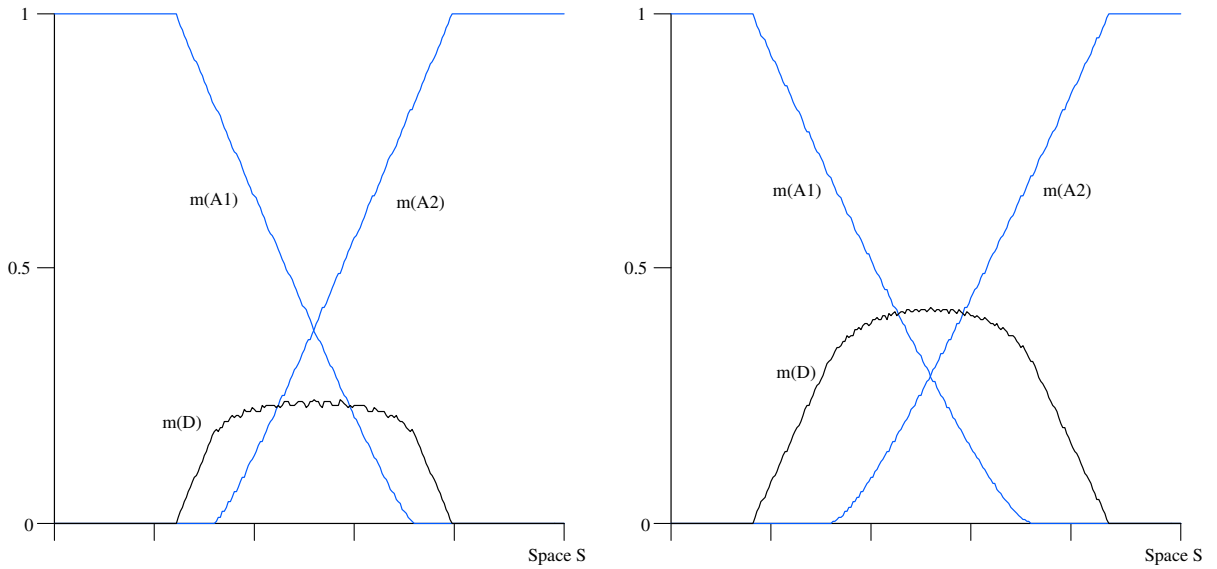

Fig. 3. Resulting mass functions on A_1 and A_2 and on D. In the second example, obtained with a larger structuring element, more imprecision is included in the mass function, resulting in a higher mass value on $D = A_1 \cup A_2$ in the ambiguity area.

3.4. Interpretation

The main interpretation of the previous development concerns introduction of imprecision. This can be done at two different levels.

(1) Let us consider that belief functions on 2^D are defined on a space of characteristics of image points. Typically, they can be the grey levels of each image (then $\mathscr{S} = [0, 255]$), as is the case of the example in Fig. 2. This is very often used when classes or objects can be characterized from their grey levels. Then, erosion or dilation by a fuzzy structuring element can be used to represent imprecision on the limits of classes on the grey level scale. This leads to a mass function on the disjunction of two classes that takes high values in the ambiguity area (i.e. on the grey levels that are intermediate between those of the two classes). This is illustrated for instance in Fig. 3. Fusion of several images will then help in solving the ambiguity between both classes in this area. An example will be shown in Section 5.8.

(2) Now, if we consider that belief functions of each subset of D are defined directly on the image space ($\mathscr{S} = \mathbb{Z}^2$ or $\mathbb{Z}^3$), then they are endowed with a spatial meaning, which is the basic information in images. In this case, spatial imprecision in the delineation of classes or objects is introduced using a fuzzy structuring element defined on the image space. An example is provided by the images (a) and (b) in Fig. 1 and will be developed in Section 5.7. Appropriate choices of the structuring element allow propagating information in a controlled way. For instance, the structuring element can represent imprecision due to registration, and can be derived from an estimation of the possible errors in the estimation of geometric parameters for instance [50]. More generally, the structuring element should introduce all prior (or learned) knowledge we may have on the imprecision attached to the problem at hand. Fuzzy structuring elements can be appropriate for this aim. Also a contextual spatial information is introduced. For instance, if the plausibility that a point belongs to a class is high, then the effect of dilation will be to increase the plausibility that its neighbors belong to the same class. In that sense, the proposed approach constitutes a new formalism for introducing spatial context in image fusion. Compared to Markov random fields in a probabilistic framework, it has the advantages of a better control of the spatial extent of the influence of operations, using an appropriate representation of imprecision. Moreover, it allows dealing with disjunctions, which are difficult to handle in a probabilistic framework.

The choice of the morphological operations has little consequences from a theoretical point of view, as soon as they satisfy the properties of duality and extensivity/anti-extensivity (hence the choice of dual versions of the operators in the fuzzy case, and of structuring elements such that $v(O) = 1$). However, from a practical point of view, important aspects should be considered. Since we have $\gamma_v(\mu) \geqslant \varepsilon_v(\mu)$ and $\varphi_v(\mu) \leqslant \delta_v(\mu)$, using opening and closing instead of erosion and dilation has globally less effect on the transformed mass functions. However, since they are filters in a morphological sense (increasing and idempotent operators), they have an additional effect of reducing noise in the first mass function estimate. This will be illustrated in Section 5.7. This effect can be interesting for instance in the case where the initial estimates are obtained experimentally in a non-parametric way. Another point concerns the choice of the structuring element, which has a direct influence on the level of imprecision in the resulting mass function (in particular on $m(D)$, as illustrated in Fig. 3). Its extent should be defined according to the imprecision to be introduced. It can be based on prior information (often available from the characteristics of the acquisitions and of the images), or on a learning procedure. Its influence will be further illustrated in Sections 5.7 and 5.8.

3.5. Consequences on the combination using Dempster's rule

Applying the proposed method in a fusion process using Dempster's rule has several consequences. At the modeling level, the introduction of imprecision using fuzzy morphological operators enlarges the belief intervals, as expected from a more imprecise mass function. On the other hand, the introduction of imprecision related to each source prior to the combination reduces the conflict between sources. This imprecision is translated in terms of disjunction of hypotheses and therefore increases ambiguity on each source, which will be solved thanks to the conjunctive behavior of the combination operator. When combining two images that carry information on different classes, say A and $\overline{A}$ for the first image, B and $\overline{B}$ for the second one, then using the belief functions derived from morphological transforms leads to more focal elements after combination. This is important in the sense that ambiguity between classes is therefore better represented, in particular via the disjunctions. This leads to a more complete model, where more features of the information are represented (not only information on the classes themselves, but also on their ambiguity). Decision can then be taken with more information. These fusion aspects will be further detailed in Section 5.

4. Extension to more than two focal elements

In this section, we extend the method to the case where the initial estimate m_0 has more than two disjoint focal elements. For the sake of clarity, let us first detail the example of three disjoint focal elements A_1, A_2, A_3. We assume that we have an initial estimate m_0 such that $m_0(A_1) + m_0(A_2) + m_0(A_3) = 1$ (known for instance from a probabilistic or fuzzy method). Let v be the structuring element representing the imprecision to be introduced in m_0 (v can be fuzzy or crisp). Let us note that all focal elements have to be processed in the same way, using the same structuring element (simple counter-examples can be found for which consistency of belief functions would be lost otherwise, as in Fig. 4).

From m_0 and v, we then define:

$$\forall i, \quad Bel(A_i) = \varepsilon_v(m_0(A_i)), Pls(A_i) = \delta_v(m_0(A_i)). \tag{24}$$

In order to satisfy duality of belief functions (Eq. (10)), we have to define the belief of disjunctions as

$$Bel(A_1 \cup A_2) = 1 - Pls(A_3) = \varepsilon_v(1 - m_0(A_3)) = \varepsilon_v(m_0(A_1) + m_0(A_2)) \tag{25}$$

and similar expressions for $Bel(A_1 \cup A_3)$ and $Bel(A_2 \cup A_3)$. The derived mass function, according to Eq. (9), is then:

$$\forall i, \quad m(A_i) = Bel(A_i) = \varepsilon_v(m_0(A_i)), \tag{26}$$

$$\forall i \neq j, \quad m(A_i \cup A_j) = \varepsilon_v(m_0(A_i) + m_0(A_j)) - \varepsilon_v(m_0(A_i)) - \varepsilon_v(m_0(A_j)). \tag{27}$$

The proof of the following results requires a simple technical lemma.

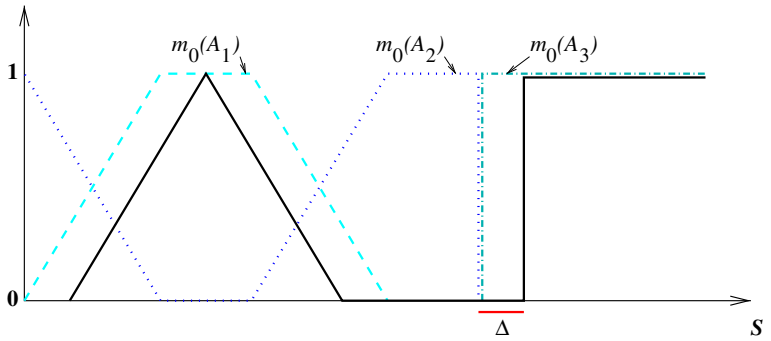

Fig. 4. An example with three initial mass functions on a 1D space. The first two are eroded with the same structuring element, while the last one is not transformed. The plain black line corresponds to $1 - \delta_v(m_0(A_2))$. Computing $m(A_1 \cup A_3) = 1 - \delta_v(m_0(A_2)) - \varepsilon_v(m_0(A_1)) - m_0(A_3)$ leads to a negative value in the area of $\mathscr{S}$ indicated by Δ, which is inconsistent.

Lemma 2. *For two functions f and g defined over the same space $\mathscr{S}$, the following property holds*:

$$\inf_{x\in\mathscr{S}}[f(x) + g(x)] \geqslant \inf_{x\in\mathscr{S}} f(x) + \inf_{x\in\mathscr{S}} g(x). \tag{28}$$

Proof. The proof of this lemma is straightforward: $\forall y \in \mathscr{S}, \inf_{x\in\mathscr{S}} f(x) \leqslant f(y)$ and $\inf_{x\in\mathscr{S}} g(x) \leqslant g(y)$, therefore $\inf_{x\in\mathscr{S}} f(x) + \inf_{x\in\mathscr{S}} g(x) \leqslant f(y) + g(y)$ and $\inf_{x\in\mathscr{S}} f(x) + \inf_{x\in\mathscr{S}} g(x) \leqslant \inf_{y\in\mathscr{S}}[f(y) + g(y)]$. □

Theorem 3. *In the case of three disjoint focal elements A_1, A_2, A_3, and for a* crisp *structuring element v, defining masses on A_i as erosions of the initial normalized masses leads to masses on disjunctions of two hypotheses that are consistent* (*i.e. take values in* [0, 1]).

Proof. Assume a normalized initial mass function m_0 on the A_i:

$$m_0(A_1) + m_0(A_2) + m_0(A_3) = 1.$$

We note $m_0(A_i) = \mu_i$.

As proposed in this paper, we define a belief function taking into account imprecision (represented by a structuring element v) as

$$Bel(A_i) = m(A_i) = \varepsilon_v(\mu_i).$$

We also define $Pls(A_i) = \delta_v(\mu_i)$, by choosing a dual pair of erosion and dilation.

Then we derive the masses on disjunctions of two hypotheses from their belief value. For instance for $A_1 \cup A_2$, we have

$$Bel(A_1 \cup A_2) = m(A_1) + m(A_2) + m(A_1 \cup A_2) = 1 - Pls(A_3) = 1 - \delta_v(\mu_3),$$

and therefore

$$m(A_1 \cup A_2) = 1 - \delta_v(\mu_3) - \varepsilon_v(\mu_1) - \varepsilon_v(\mu_2).$$

If v is a binary structuring element, from $\varepsilon_v(\mu_i)(x) = \inf_{y\in v_x} \mu_i(y)$ and from Lemma 2, we derive

$$\varepsilon_v(\mu_1) + \varepsilon_v(\mu_2) \leqslant \varepsilon_v(\mu_1 + \mu_2)$$

Since $1 - \delta_v(\mu_3) = \varepsilon_v(\mu_1 + \mu_2)$, this shows that $m(A_1 \cup A_2) \geqslant 0$. Since all erosion values are in $[0, 1]$, we also have $m(A_1 \cup A_2) \leqslant 1$, and

$$m(A_1 \cup A_2) \in [0, 1].$$

The same reasoning holds for any disjunction of two hypotheses. □

Let us denote $\mathscr{M} = \sum_{A\subset D, A\neq D} m(A)$ ($\mathscr{M} \geqslant 0$). Since this sum is not always in $[0, 1]$ (it is difficult to exhibit realistic examples, but very particular situations may lead to $\mathscr{M} > 1$), two solutions are possible for defining $m(D)$. The first one consists in setting $m(D) = 0$, and normalizing all other masses by $\mathscr{M}$. This solution is

adapted to cases where we have no information on a global reliability or global ignorance on the images (this is often the case in medical imaging for instance). The second solution consists in setting $m(D) = 1 - \mathscr{M}$ if $\mathscr{M} \leqslant 1$. Both solutions guarantee that $\sum_{A \subseteq D} m(D) = 1$. Since m is then a mass functions with all its properties, the belief function, which satisfies Eq. (9) according to our construction, also satisfies Eq. (8). Eq. (11) is satisfied too (this is directly derived from Eq. (12)).

Let us now consider the case of a fuzzy structuring element. We prove a somewhat less general result, by assuming that ambiguity occurs between at most two hypotheses.

Theorem 4. *In the case of three initial focal elements A_1, A_2, A_3, and for a* fuzzy *structuring element v, if there is locally ambiguity between at most two hypotheses, expressed formally as*

$$\exists i, j, i \neq j, \quad \delta_{Supp(v)}(Supp(\mu_i)) \cap \delta_{Supp(v)}(Supp(\mu_j)) = \emptyset, \tag{29}$$

where $\mu_i = m_0(A_i)$ and $Supp(\mu) = \{x \in \mathscr{S}, \mu(x) > 0\}$, then, using the proposed construction, masses on disjunctions of two hypotheses are consistent (i.e. take values in $[0,1]$), $m(D) = 0$, and $\sum_{A \subseteq D} m(A) = 1$. Thus all required properties are satisfied.

The condition expressed in Eq. (29) is illustrated in Fig. 5.

Proof. We use the same notations as before, and assume $i = 1$ and $j = 3$ (without loss of generality). Since for any t-norm chosen in the definition of the dilation, we have

$$Supp(\delta_v(\mu)) \subseteq \delta_{Supp(v)}(Supp(\mu))$$

(with an equality for some t-norms such as minimum or product), the condition expressed in Eq. (29) implies that

$$Supp(\delta_v(\mu_1)) \cap Supp(\delta_v(\mu_3)) = \emptyset$$

and

$$Supp(\delta_v(\mu_1)) \cap Supp(\varepsilon_v(\mu_3)) = \emptyset.$$

Let us compute $m(A_2 \cup A_3)$:

$$m(A_2 \cup A_3) = 1 - \delta_v(\mu_1) - \varepsilon_v(\mu_2) - \varepsilon_v(\mu_3)$$

- At points of $\mathscr{S}$ where $\delta_v(\mu_1) = 0$, we have

$$m(A_2 \cup A_3) = 1 - \varepsilon_v(\mu_2) - \varepsilon_v(\mu_3)$$

Since $\varepsilon \leqslant Id$, $0 \leqslant \varepsilon_v(\mu_2) + \varepsilon_v(\mu_3) \leqslant \mu_2 + \mu_3 \leqslant 1$, and $0 \leqslant m(A_2 \cup A_3) \leqslant 1$.

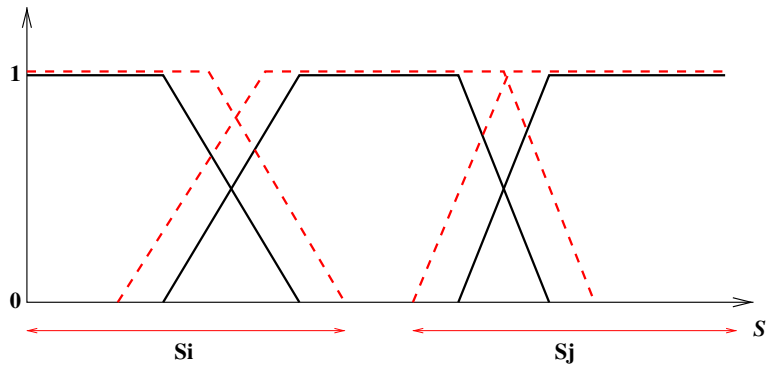

Fig. 5. Three initial mass functions (plain lines) defined on a 1D space, in the case of three hypotheses, where the first and the third one are separated according to Eq. (29), i.e. there is no ambiguity between these two classes, and they remain separated after dilation (dashed lines), as shown by their supports **Si** and **Sj**.

- At each point of $\mathscr{S}$ where $\delta_v(\mu_1) \neq 0$, then $\varepsilon(\mu_3) = 0$, $\mu_3 = 0$ and $\mu_2 = 1 - \mu_1$, according to Eq. (29), and this holds at least in a neighborhood of size $Supp(v)$ of the point. Therefore $\varepsilon_v(\mu_2) = \varepsilon_v(1 - \mu_1) = 1 - \delta_v(\mu_1)$ and $m(A_2 \cup A_3) = 0$.

  A similar reasoning applies to $m(A_1 \cup A_2)$.
  As for $m(A_1 \cup A_3)$, we have

  $$m(A_1 \cup A_3) = 1 - \delta_v(\mu_2) - \varepsilon_v(\mu_1) - \varepsilon_v(\mu_3)$$

  The condition in Eq. (29) implies that the supports of $\varepsilon_v(\mu_1)$ and $\varepsilon_v(\mu_3)$ are disjoint, therefore at each point, at least one of the values of the erosion is 0. Let us assume that $\varepsilon_v(\mu_1) = 0$. The same reasoning as above leads to $m(A_1 \cup A_3) = 0$. The case where $\varepsilon_v(\mu_3) = 0$ leads to the same result.
  Let us now compute $m(D) = m(A_1 \cup A_2 \cup A_3)$.

  $$\begin{aligned} m(D) &= 1 - m(A_1) - m(A_2) - m(A_3) - m(A_1 \cup A_2) - m(A_2 \cup A_3) - m(A_1 \cup A_3) \\ &= \delta_v(\mu_1) + \delta_v(\mu_3) + \varepsilon_v(\mu_2) - 1, \end{aligned}$$

  since $m(A_1 \cup A_3) = 0$.

- At each point of $\mathscr{S}$ where $\delta_v(\mu_1) = 0$, using the same reasoning as above, we have

  $$\begin{aligned} m(D) &= \delta_v(\mu_3) + \varepsilon_v(\mu_2) - 1 \\ &= \delta_v(\mu_3) + \varepsilon_v(1 - \mu_3) - 1 \\ &= \delta_v(\mu_3) + 1 - \delta_v(\mu_3) - 1 = 0. \end{aligned}$$

- At each point of $\mathscr{S}$ where $\delta_v(\mu_1) \neq 0$, we have $\delta_v(\mu_3) = 0$, and:

  $$\begin{aligned} m(D) &= \delta_v(\mu_1) + \varepsilon_v(\mu_2) - 1 \\ &= \delta_v(\mu_1) + \varepsilon_v(1 - \mu_1) - 1 \\ &= \delta_v(\mu_1) + 1 - \delta_v(\mu_1) - 1 = 0. \end{aligned}$$

This shows that we always have $m(D) = 0$, and $\sum_{A \subseteq D} m(A) = 1$. Thus m is a mass function with all properties. Since *Bel* is linked to m by Eq. (9), it follows that all properties of belief functions are satisfied too, in particular Eq. (8). □

Theorem 4 extends to the case of any number n of hypotheses, as follows.

Theorem 5. *Let m_0 be a normalized mass function having n focal elements $A_1, \ldots, A_n$, and denote $\mu_i = m_0(A_i)$. The proposed construction, using a* fuzzy *structuring element v, is consistent under the condition that the functions μ_i are "ordered" such that*:

$$\begin{aligned} &\forall j, j \geqslant 3, \quad \delta_{Supp(v)}(Supp(\mu_1)) \cap \delta_{Supp(v)}(Supp(\mu_j)) = \emptyset, \\ &\forall i,\ 1 < i < n,\ \forall j, j \notin [i-1, i+1], \quad \delta_{Supp(v)}(Supp(\mu_i)) \cap \delta_{Supp(v)}(Supp(\mu_j)) = \emptyset, \\ &\forall j,\ j \leqslant n-2, \quad \delta_{Supp(v)}(Supp(\mu_n)) \cap \delta_{Supp(v)}(Supp(\mu_j)) = \emptyset. \end{aligned}$$

Under this condition, we have

$$\begin{aligned} &\forall i, j,\ i \neq j, \quad 0 \leqslant m(A_i \cup A_j) \leqslant 1, \\ &\forall i, j,\ |i - j| > 1, \quad m(A_i \cup A_j) = 0, \\ &\forall I \subseteq \{1, \ldots, n\}, \quad |I| \geqslant 3, m\left(\bigcup_{i \in I} A_i\right) = 0. \end{aligned}$$

This means that ambiguity between hypotheses can only occur between "successive" hypotheses, according to the defined order. In particular, $m(D) = 0$.

Proof. The proof is similar as the one of Theorem 4. □

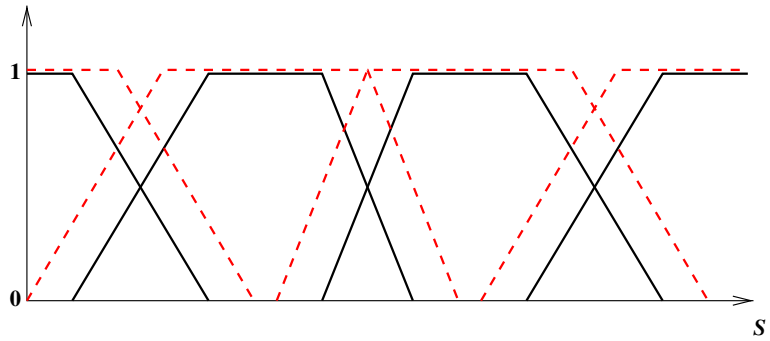

Fig. 6. Illustration of the condition expressed in Theorem 5: each initial mass function (plain lines) presents ambiguity with at most the preceding one and the following one. The support of its dilation (dashed lines) intersects at most the supports of the dilations of the two neighboring functions.

Fig. 6 illustrates the condition expressed in this result.

In the case where the initial focal elements are not disjoint, the same construction can be performed by assigning a null mass to the intersections of the focal elements and to the disjunctions involving these intersections. However, we are mainly interested in initial disjoint focal elements, since it corresponds to most learning methods used in image processing.

As a summary, the following sequence reviews the main steps of our approach:

(1) normalized initial mass m_0;
(2) derivation of *Bel* and *Pls* on the initial focal elements (and their complements) using dual morphological operators;
(3) duality ensures Eq. (10);
(4) Eq. (12) ensures Eq. (11);
(5) derivation of the new mass function, which incorporates the imprecision represented by the structuring element used in the morphological operations (for $m(D)$, different possibilities exist);
(6) the normalization condition on D is satisfied;
(7) since *Bel* and m are linked by Eq. (9) and m satisfies all properties of a mass function, *Bel* satisfies Eq. (8).

5. Applications to image fusion

Since the theoretical development presented in Section 3 is particularly straightforward if the initial mass functions are non-zero on two complementary hypotheses, we will present several possible schemes applying this approach. A last scheme relies on a direct application of the method extended to the case where the initial mass functions have more than two focal elements.

5.1. Two hypotheses

If each image provides information on one hypothesis and its contrary, then the proposed method applies directly (Section 3). It should be noted that this hypothesis has not necessarily to be a singleton. It can also be a disjunction of classes, which is very useful for practical applications in image processing (see the example in Section 5.8).

5.2. Estimating each class or disjunction of classes against all the others

One possible scheme consists in deriving, from each image, several mass functions, where each of them has only two complementary focal elements. This amounts to increase the number of information sources, and

calls for specific image processing methods for estimating each class (or disjunction of classes) against all the others. However, this is a process that is widely used in pattern recognition methods, and, in most image processing applications, tools have been developed for extracting one type of objects from the rest of the scene. For instance, a lot of algorithms have been proposed for extracting roads, urban areas, or vegetation from satellite images. Therefore, we can derive from the output of these algorithms the required initial mass functions. One of the advantage in using this scheme is that we can process imprecision related to each image or each extraction result independently, and according to the detection algorithm that has been used. More formally, from a set of images, we derive initial mass functions m_0^i $(1 \leqslant 1 \leqslant N)$ on A_i and $\overline{A}_i$, and a structuring element v_i representing the imprecision associated with this estimate. The number of mass functions N will generally be greater than the number of images. Then a set of mass functions m^i is derived from fuzzy erosion and dilation of m_0^i by the structuring element v_i, according to Eqs. (17), (18) and (23). The fusion is performed using Dempster's rule of combination $m = \oplus_{i=1\ldots N} m^i$, from which the final decision is taken.

Note that in the case where the focal elements of the initial masses are singletons and their complementary, we recover Barnett's structure [51]. This results in particular in a linear complexity in the computation of the combination.

5.3. Successive refinements

Another possible scheme consists in performing successive refinements of the mass function. Let us assume that a first mass function m_0 is estimated from an image on A and $\overline{A}$. We first introduce the imprecision on this estimate using a fuzzy structuring element v, thus obtaining a mass m on A, $\overline{A}$ and $A \cup \overline{A}$. Then $\overline{A}$ is refined in B and $\overline{A} \setminus B$, with $B \subseteq \overline{A}$. The same process as before is applied in $\overline{A}$, and the resulting mass on B, $\overline{A} \setminus B$ and $\overline{A}$ is normalized such that the sum is equal to $m(\overline{A})$. This process is recursively applied until we get a refinement as precise as we want. The main problem with this approach is that not all subsets of D appear in the decomposition. Therefore, an appropriate order has to be chosen in such a way that the interesting disjunctions appear. For instance, let us consider a 3-class problem, i.e. $D = \{C_1, C_2, C_3\}$. If we first try to estimate C_1 against the other classes, and then refine $\overline{C}_1$, the following focal elements are obtained:

(1) first estimate: C_1, $\overline{C}_1 = \{C_2, C_3\}$,
(2) after erosion/dilation by v: C_1, $\overline{C}_1 = \{C_2, C_3\}$, D,
(3) after refinement: C_1, C_2, C_3, D,
(4) after erosion/dilation by v' (which does not need to be equal to v) of the masses on C_2 and C_3: C_1, C_2, C_3, $\{C_2, C_3\}$, D.

The disjunctions $\{C_1, C_2\}$ and $\{C_1, C_3\}$ do not appear directly in this decomposition.

Post-processing of the obtained mass function can be performed in order to overcome this problem, again using morphological operators, for instance by dilating the area of ambiguity between two classes (taken e.g. as a t-norm between the mass functions) and normalizing the result. For the previous example, $\delta_v[\top(m(C_1), m(C_2))]$ can be computed in order to derive a mass on $\{C_1, C_2\}$.

5.4. Direct method

The last scheme consists in applying directly the method extended to the case of n focal elements in the initial estimate, as presented in Section 4. Here again, each of these focal elements can be either a singleton or a disjunction of hypotheses. This scheme can also be combined for instance to the refinement scheme, in order to obtain more discrimination between classes.

5.5. Comparison between schemes

It appears that these schemes have different properties and behaviors, and therefore can be chosen depending on the application at hand.

The first scheme increases the number of sources but the complexity may be linear in the case of Barnett's structure. It allows adapting the structuring element to each type of information and to each algorithm (representation of imprecision induced by an algorithm). It is necessary to have an algorithm for extracting the information on the hypotheses of interest, but all hypotheses can be considered.

The successive refinements scheme provides a hierarchical structure, which may give rise to different levels of interpretation. However, the order in which the decomposition is performed is very important, since the resulting focal elements depend on it.

The direct method does not increase the number of sources. The same structuring element has to be used for all hypotheses (representation of global imprecision on the limits of classes or objects, that may be intrinsic to the images and does not necessarily depends on a preliminary processing algorithm). Imprecision on the initial focal elements is directly taken into account. This approach is more systematic, and needs less information in order to be applicable.

5.6. Some properties

It is interesting to note a few properties of the proposed approach on the fusion results, in particular:

- new focal elements (disjunctions) appear with the morphological operations;
- this results in a decrease of conflict with respect to the combination of the initial mass functions;
- this results also in larger belief intervals $[Bel, Pls]$;
- decision can account for the imprecision, as will be seen in the examples of Sections 5.7 and 5.8.

Let us take some simple examples to illustrate these properties. We first consider the case of two initial focal elements A and $\overline{A}$. Let us denote by a_1 and a_2 the initial masses on A in each image, and by a'_1 and a'_2 the masses on A after erosion (with $a'_1 \leqslant a_1$ and $a'_2 \leqslant a_2$), and $\bar{a}'_1$ and $\bar{a}'_2$ the masses on $\overline{A}$ after erosion (with $\bar{a}'_1 \leqslant 1 - a_1$ and $\bar{a}'_2 \leqslant 1 - a_2$).

- The focal elements after the morphological operations are $A, \overline{A}, D$.
- The conflict is equal to $a_1(1 - a_2) + a_2(1 - a_1)$ when combining the initial masses. It then becomes $a'_1\bar{a}'_2 + \bar{a}'_1 a'_2$, which is lower than the initial conflict.
- The belief interval is initially $[a_1, a_1]$ for image 1 (i.e. of length equal to zero), and then becomes $[a'_1, 1 - \bar{a}'_1]$. The same holds for the second source.
- The fusion on the initial mass functions leads to a decision in favor of A if $a_1 a_2 \geqslant (1 - a_1)(1 - a_2)$. It depends noticeably on a t-norm (product). After the morphological operations, combining the resulting mass functions leads to a decision in favor of A if $a'_1 + a'_2 - a'_1 a'_2 \geqslant \bar{a}'_1 + \bar{a}'_2 - \bar{a}'_1\bar{a}'_2$, i.e. it depends on a t-conorm (algebraic sum), which corresponds to a more cautious combination.

Let us now consider the example of two initial focal elements A and $\overline{A}$ for source 1, and B and $\overline{B}$ for source 2.

- The focal elements after combination of the initial mass functions (m_0) are A, B and $D\backslash(A \cup B)$ if $A \cap B = \emptyset$, and $A \cap B$, $A\backslash B$, $B\backslash A$ and $D\backslash A\backslash B$ if $A \cap B \neq \emptyset$. After combination of the transformed mass functions using erosions, the focal elements are A, B, $\overline{A}$, $\overline{B}$, $D\backslash(A \cup B)$ and D if $A \cap B = \emptyset$, and A, B, $\overline{A}$, $\overline{B}$, $A \cap B$, $A\backslash B$, $B\backslash A$, and $D\backslash(A \cup B)$ and D if $A \cap B \neq \emptyset$ (more focal elements appear).
- Again the conflict is reduced after the erosions.
- Decision rules also change, but the expressions are not as simple as in the previous example.

5.7. Example on a synthetic image

Let us now illustrate the proposed approach in the spatial domain. We consider a synthetic image, and two noisy observations of it, that are considered as the two sources of information (see Fig. 7). The image contains two classes (the white square C_1, and the background C_2), the frame of discernment being simply

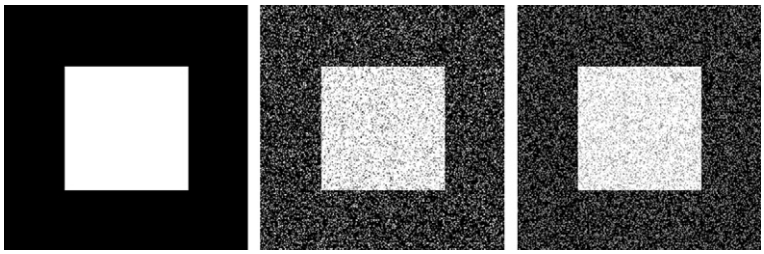

Fig. 7. Original scene (with two classes: the white square and the background) and two noisy observations, simulating two information sources, and defining $m_0^1(C_1)$ and $m_0^2(C_1)$.

$D = \{C_1, C_2\}$. The ideal decision image should be as close as possible to this image. We use directly the grey levels of each pixel, normalized on the $[0, 1]$ scale, as mass values at this pixel. The two noisy observations provide directly the initial masses on C_1, $m_0^1(C_1)$ and $m_0^2(C_1)$, and there complement the initial masses on C_2, $m_0^1(C_2) = 1 - m_0^1(C_1)$ and $m_0^2(C_2) = 1 - m_0^2(C_1)$ (Fig. 8).

Fig. 9 illustrates the decision taken on each image separately, without fusion. The decision images are in both cases noisy and do not show a clear separation between the two classes.

Applying Dempster combination rule on the initial mass functions leads to the mass functions and decision images displayed in Fig. 10. Although there is a small improvement due to the fusion, leading to a slightly less noisy result, the final decision is still not satisfactory.

Let us now apply morphological erosion and dilation, in the spatial domain, on the initial mass functions. This leads to belief and plausibility of each class, as shown in Fig. 11 for the first image, and in Fig. 12 for the second image. It can be observed that erosion induces noise removal in the background, while dilation has a similar effect in the white square.

The mass values on D are illustrated in Fig. 13 for both images. The obtained values are high in particular in the intermediate area between the two classes, which is consistent with the fact that the boundary is imprecise, and therefore adequately represented by high values on D.

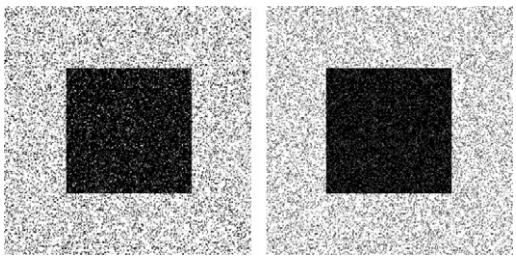

Fig. 8. Masses for the second class for the two sources $m_0^1(C_2) = 1 - m_0^1(C_1)$ and $m_0^2(C_2) = 1 - m_0^2(C_1)$.

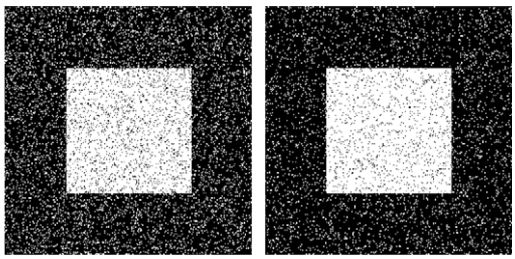

Fig. 9. Decision without fusion, on source 1 (left) and on source 2 (right).

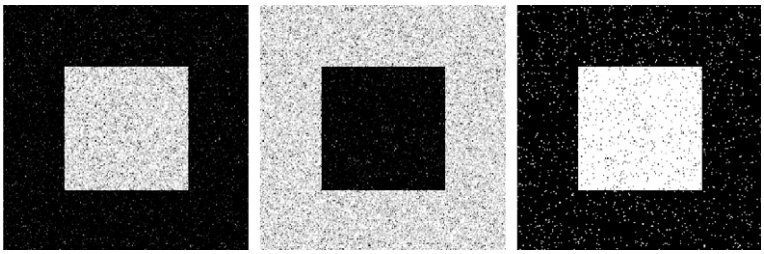

Fig. 10. Fusion of m_0^1 and m_0^2: resulting masses for C_1 and C_2 and decision after fusion.

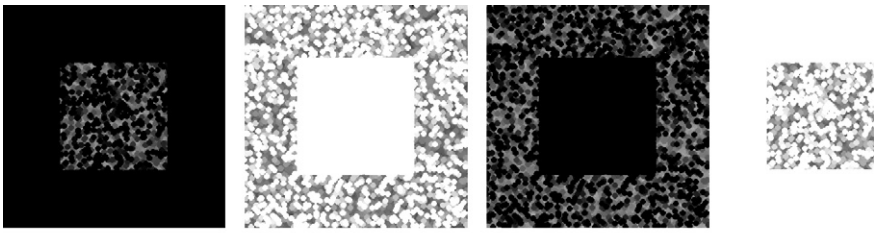

Fig. 11. Introducing imprecision with mathematical morphology for source 1. (a) $Bel^1(C_1)$ from erosion of $m_0^1(C_1)$. (b) $Pls^1(C_1)$ from dilation of $m_0^1(C_1)$. (c) $Bel^1(C_2)$ from erosion of $m_0^1(C_2)$. (d) $Pls^1(C_2)$ from dilation of $m_0^1(C_2)$.

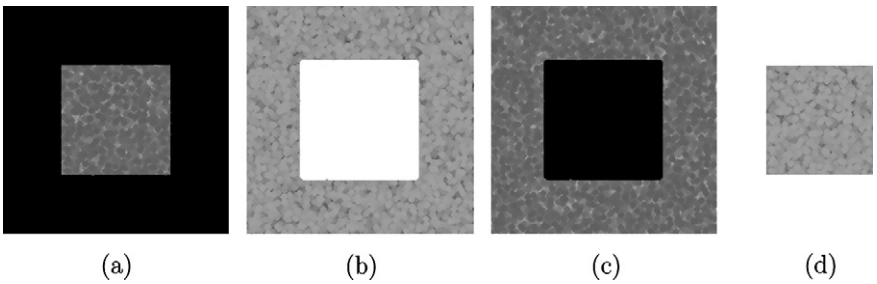

Fig. 12. Introducing imprecision with mathematical morphology using erosion and dilation for source 2.

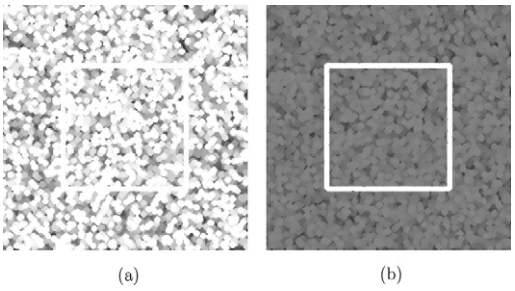

Fig. 13. $m^1(D)$ (a) and $m^2(D)$ (b). Highest values are obtained around the boundary between both classes, representing the imprecision of the limit.

The fusion, using Dempster's rule, leads to the masses on C_1, C_2 and D and the decision image illustrated in Fig. 14. The results are much better thanks to the morphological operations. The final decision, taking according to the highest mass value at each point (i.e. a point x is assigned to the white square if $m(C_1)(x) > m(C_2)(x)$

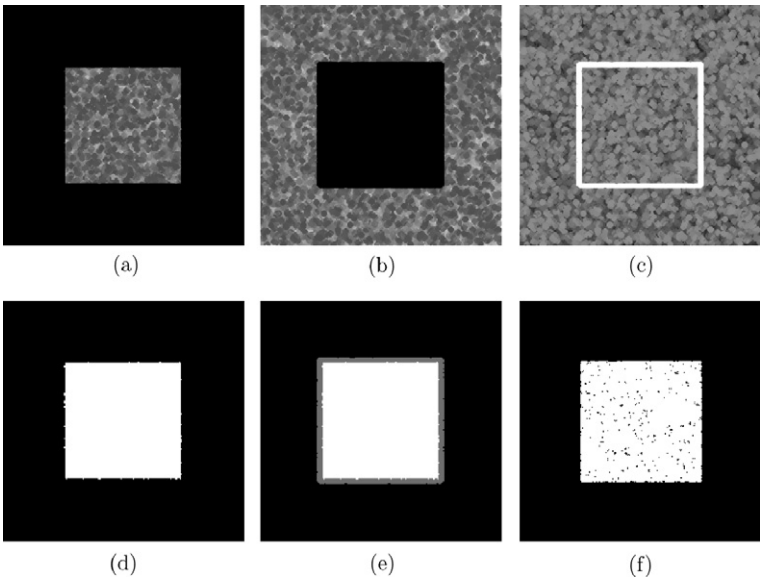

Fig. 14. Fusion of m^1 and m^2. Resulting masses for C_1 (a), C_2 (b) and D (c). (d) Decision after fusion by choosing at each point the class with the highest mass value. (e) Decision taking into account the imprecision at the boundary: points with high values of $m(D)$ (in medium grey) are too ambiguous to be assigned to any of the two classes. (f) Result obtained by first filtering the images and then combining them and making decision.

and to the background otherwise), is much closer to the initial image. Only a few irregularities appear on the boundary between the two classes.

The imprecision at the boundary can be taken into account in the decision, by not assigning points with a high value of $m(D)$ to one of the two classes. This is illustrated in Fig. 14e.

To show experimentally the benefit of the proposed approach, the images have been first filtered using a spatial filter, and then combined before making the decision (as in Fig. 10). The result, obtained with a median filter and displayed in Fig. 14 (f), is spatially less consistent than the one obtained with the proposed approach. Similar results are observed using other filters (local average or morphological filters for instance).

The size of the structuring element directly influences the extent of the spatial imprecision that is taken into account, and is cleary visible on $m(D)$. For instance, using a smaller (respectively larger) structuring element results in a reduced (respectively extended) imprecision area between the two classes. This also leads to a more restricted (respectively stronger) filtering effect on the mass functions. This is illustrated in Fig. 15. The shape of the structuring element also has an influence. Here isotropic structuring elements are chosen. But if the type of imprecision to be taken into account has privileged directions, the structuring element can be adapted (for instance using segments in these directions). This is a classical feature of mathematical morphology.

Other dual pairs of morphological operators can be used as well, such as opening and closing. Figs. 16–19 represent the same steps as previously, by replacing erosion by opening and dilation by closing. Now the final decision (Fig. 19d) has a regular boundary, and is almost everywhere even better than the one obtained with erosion and dilation. This is due to the filtering effect of opening and closing operators. Note that the corners of the square are slightly smoothed too, and the limit between the two classes is not as good in these areas as using erosion and dilation.

This very simple example illustrates the interest of the proposed approach to represent and overcome spatial imprecision on a classification and on the boundary between classes.

5.8. Application on medical images

We now illustrate the proposed approach on a simple example in medical imaging, addressing the problem of multi-source brain image classification. Images are acquired using magnetic resonance imaging (MRI) using

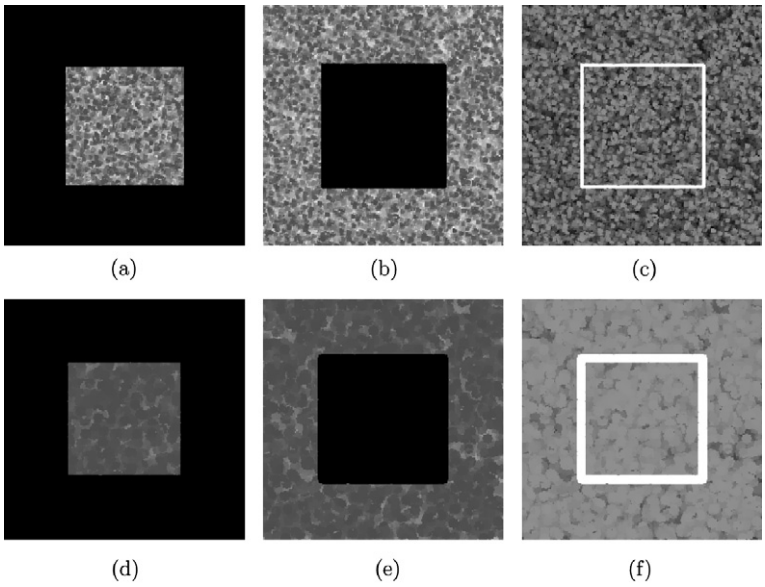

Fig. 15. Resulting masses for C_1 (a,d), C_2 (b,e) and D (c,f) after fusion, using different structuring elements. (a–c) Smaller structuring element. (d–f) Larger structuring element.

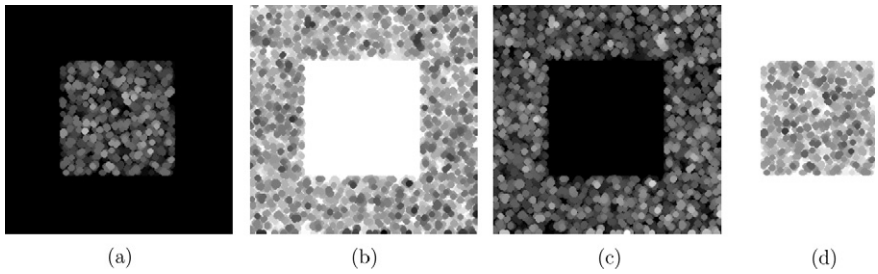

Fig. 16. Introducing imprecision with mathematical morphology for source 1. (a) $Bel^1(C_1)$ from opening of $m_0^1(C_1)$. (b) $Pls^1(C_1)$ from closing of $m_0^1(C_1)$. (c) $Bel^1(C_2)$ from opening of $m_0^1(C_2)$. (d) $Pls^1(C_2)$ from closing of $m_0^1(C_2)$.

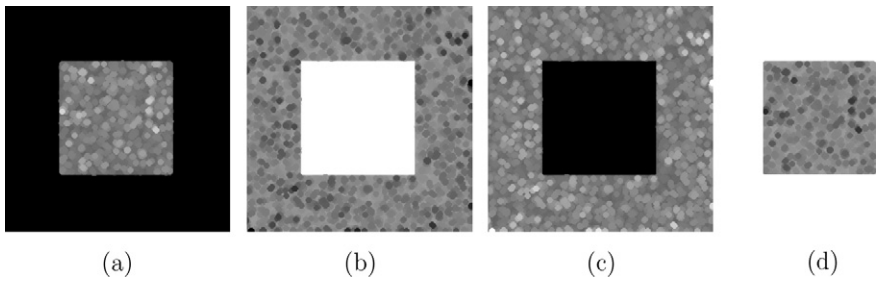

Fig. 17. Introducing imprecision with mathematical morphology using opening and closing for source 2.

two different sets of acquisition parameters (dual-echo MRI). These images constitute the two sources to be combined in order to improve the classification. In this application, we consider pathological brains, as previously addressed in [20], for which the proposed method using morphological operations will prove its interest.

Fig. 20 shows an example of initial images. The first echo does not allow seeing the pathology, but the ventricles and the cerebro-spinal-fluid (CSF) are well delineated and separated from the rest of the brain. The sec-

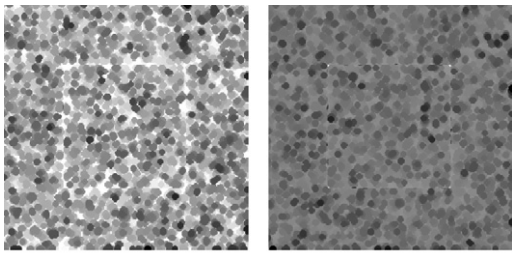

(a) (b)

Fig. 18. $m^1(D)$ (a) and $m^2(D)$ (b), obtained after opening and closing.

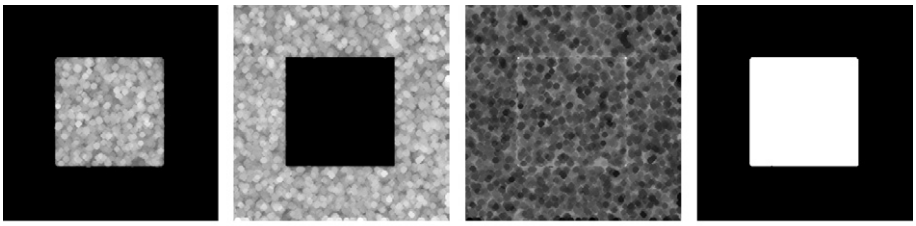

(a) (b) (c) (d)

Fig. 19. Fusion of m_0^1 and m_0^2 obtained by opening. Resulting masses for C_1 (a), C_2 (b) and D (c), and decision after fusion (d). Compared to the results obtained with erosion and dilation, opening and closing achieve an additional filtering effect, which results in a smoother boundary between the two classes in the decision image (however, corners of the square are smoothed too).

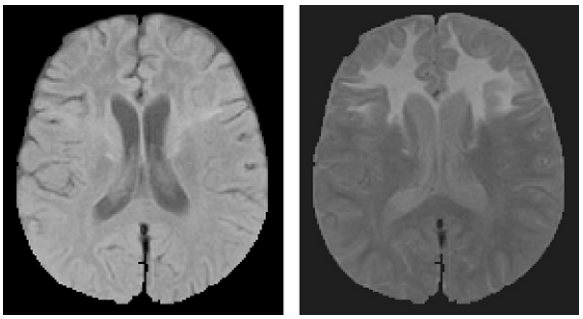

Fig. 20. One axial slice of the original dual-echo MR acquisitions. The pathology is only visible in the second echo (bright area) – Courtesy Professor Catherine Adamsbaum, Saint Vincent de Paul Hospital, Paris.

ond echo shows a bright area corresponding to the pathology. The thickness of the slices results in a lot of partial volume effect around the pathology, evidenced by intermediate grey levels. Ventricles and CSF are difficult to separate from the brain in the second image.

These differences between the images also appear on the grey level histograms (Fig. 21). The first one has two peaks, one corresponding to the ventricles and the CSF, and the second one to the other brain tissues. The second histogram shows generally lower grey levels. The first peak corresponds to the brain and the ventricles and CSF, while the second one clearly shows the characteristic grey levels of the pathology.

These observations lead to a simple modeling of the classification problem. Three classes can be exhibited: C_1 corresponds to the normal brain tissues, C_2 to the ventricles and CSF, and C_3 to the pathology. The focal elements are $\{C_1, C_3\}$ and C_2 for the first image, and $\{C_1, C_2\}$ and C_3 for the second image. Initial masses are defined from the histogram as in [23], on the grey level space. They are shown in Fig. 22.

The combination of these mass functions using Dempster's rule leads to focal elements reduced to singletons. In this example, the ambiguity between classes in each image is solved by the information contained in

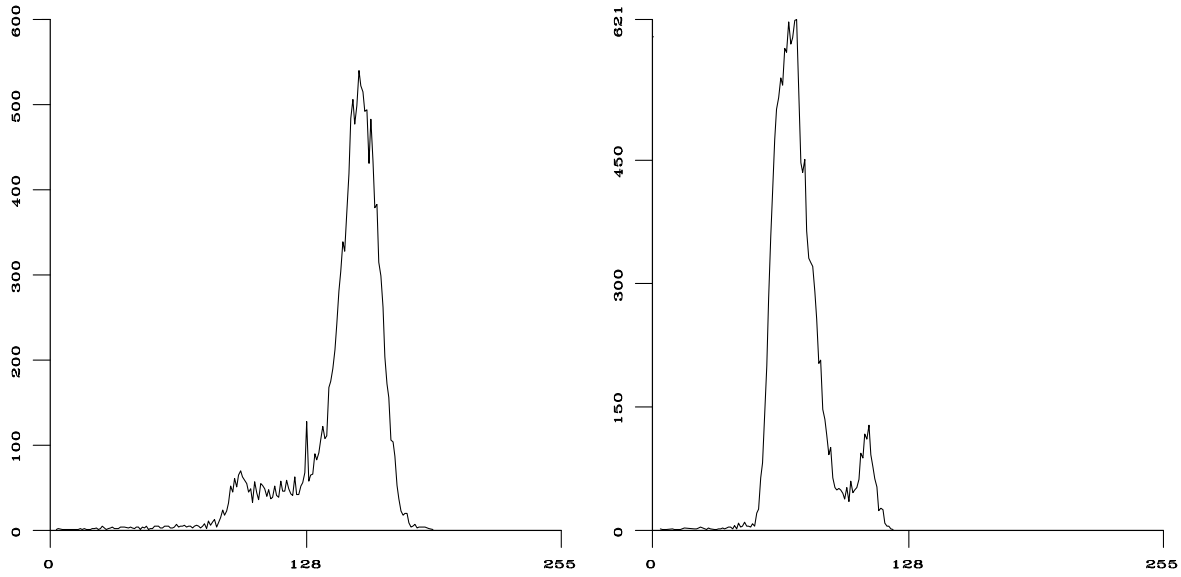

Fig. 21. Grey level histograms of two initial images (without the background).

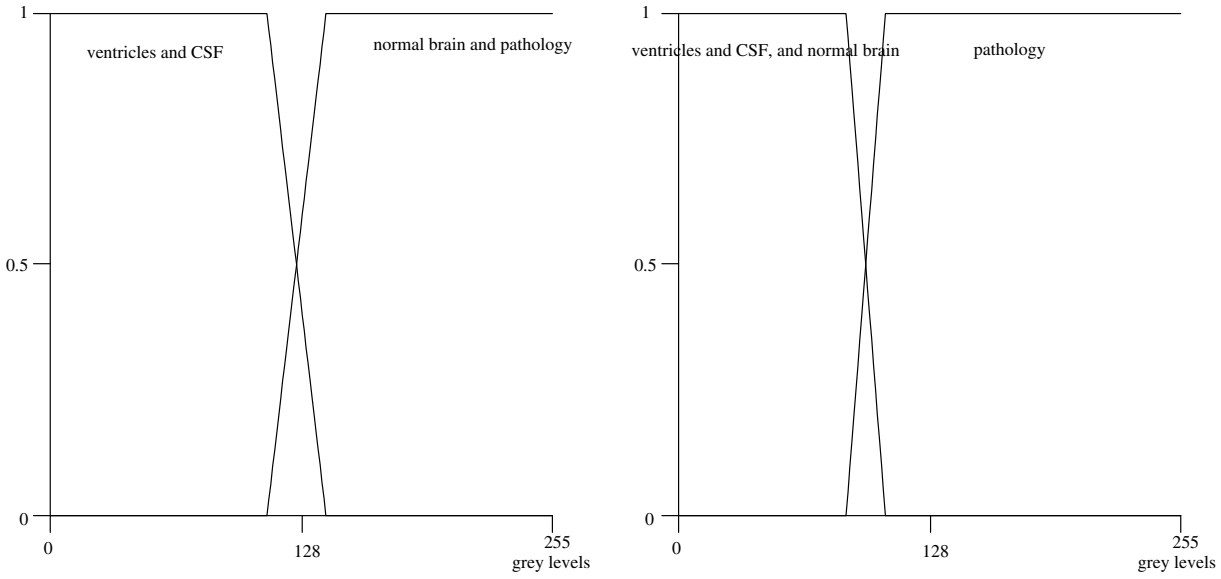

Fig. 22. Initial mass functions for the two images.

the other image. The decision image is shown in Fig. 23. In this result, the pathology class only includes pixels composed of almost pure pathological tissue. Pixels in the intermediate area, composed of a mixture of pathological and normal tissues are to a large part assigned to the normal brain class. Note that the boundary between the two classes depends on the estimation of the initial mass functions, which can be seen as a drawback. This problem is overcome by modeling explicitly imprecision between classes using mathematical morphology.

Let us now apply the proposed approach on these initial mass functions. The size of the erosion is derived from the range of ambiguous grey levels between classes in the histograms. Erosions and dilations are applied in the grey level domain. The results of erosion of the initial masses and the mass on D are displayed in Fig. 24.

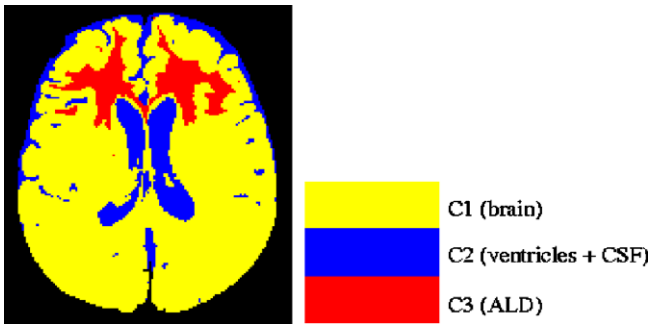

Fig. 23. Decision image based on the fusion of the initial masses.

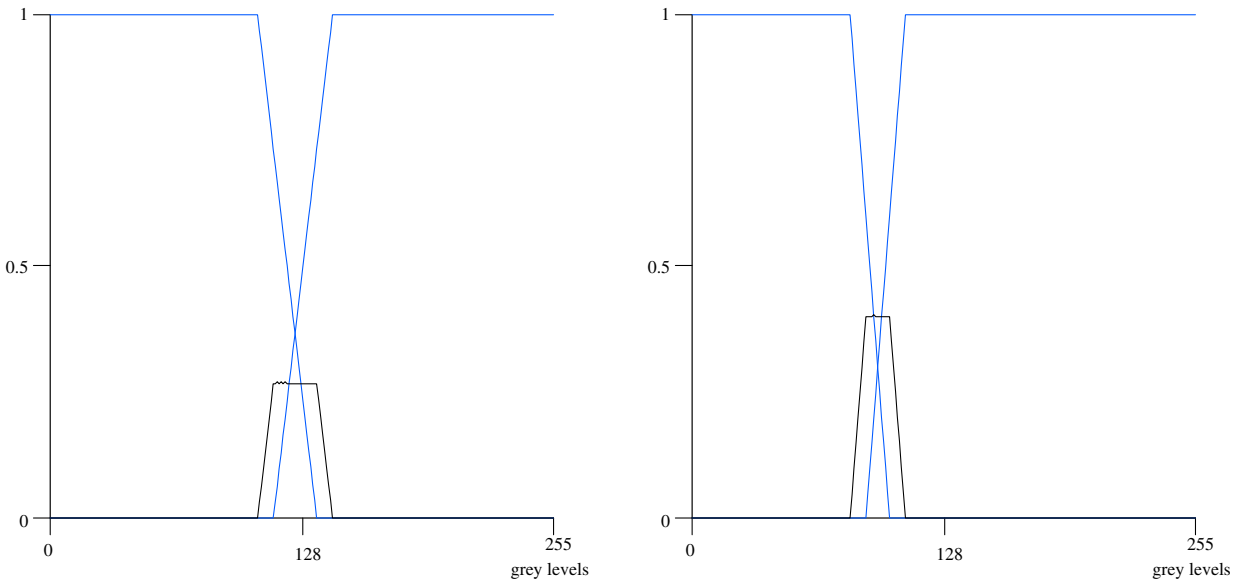

Fig. 24. Eroded mass functions and mass on D for the two images.

Now the combination with Dempster's rule provides focal elements that also include disjunctions, as shown by the intersection table (Table 1).

Fig. 25 illustrates three types of decision images:

(1) The first one is based on maximum of pignistic probability rule [52]. It does not show much difference with respect to Fig. 23.
(2) The second decision rule is based on maximum of belief over the singletons. The result includes more of the intermediate region in the pathology area. Also the cortical sulci, which are thin with respect to the slice thickness and therefore also prone to partial volume effect, are better delineated and included in the CSF class. This constitutes an improvement.
(3) The third decision is based on maximum of belief over all hypotheses (including disjunctions, except D). This means that a decision is taken in favor of a singleton only if the masses on disjunctions involving this class and on other singletons composing these disjunctions are equal to 0. It is the most interesting one, since the results show that the use of mathematical morphology operators allow modeling explicitly the imprecision in grey levels due to the partial volume effect. The decision in favor of $\{C_1, C_3\}$ clearly shows the intermediate area around the pathology, which is consistent with the medical interpretation. Similarly, the sulci are included in the decision area for $\{C_1, C_2\}$ (i.e. mixture of brain and CSF), which is

Table 1
Intersections between the focal elements of the two sources after erosion

	C_2	$\{C_1, C_3\}$	D
$\{C_1, C_2\}$	C_2	C_1	$\{C_1, C_2\}$
C_3	$\emptyset$	C_3	C_3
D	C_2	$\{C_1, C_3\}$	D

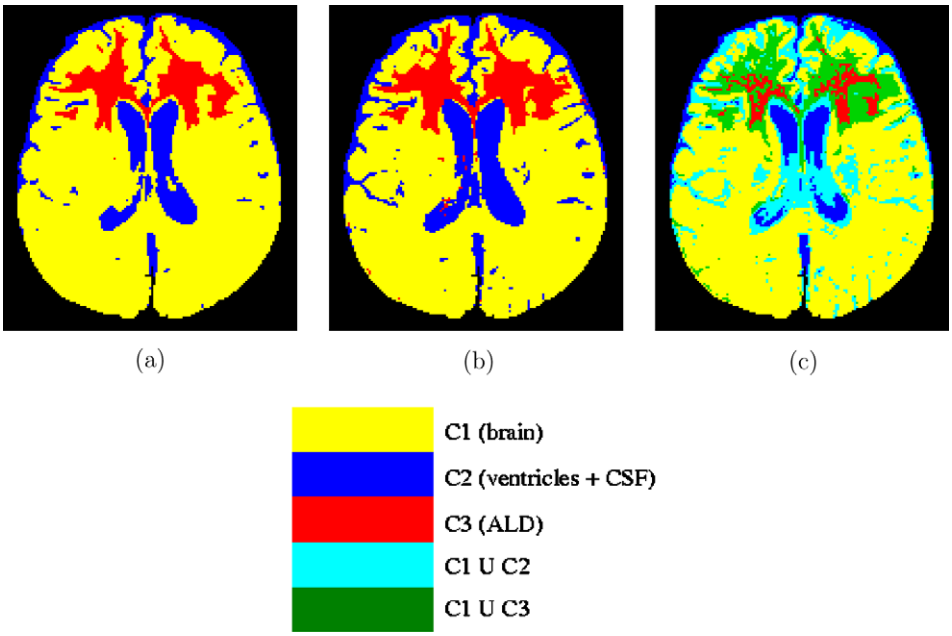

Fig. 25. Decision images based on the fusion of the masses obtained after morphological operations. (a) Decision based on maximum of pignistic probability. (b) Decision based on maximum of belief over all singletons. (c) Decision based on maximum of belief over all subsets of D except D. The intermediate area between pathology and normal brain highlights the partial volume effect. The intermediate area between CSF and normal brain illustrates the influence of slice thickness on narrow structures such as cortical sulci.

again consistent. Non-ambiguous regions are correctly assigned to singleton hypotheses. Let us detail this decision rule around the pathology (C_3). There is a smooth transition between pure pathological tissues and pure non-pathological tissues. Hence the potential decisions in these regions are C_1, C_3, $\{C_1, C_3\}$. The maximum of belief leads to making decisions in favor of:

- C_1 if $m(C_3) = m(\{C_1, C_3\}) = 0$;
- C_3 if $m(C_1) = m(\{C_1, C_3\}) = 0$;
- $\{C_1, C_3\}$ if $m(\{C_1, C_3\}) \neq 0$ or $(m(C_3) \neq 0$ and $m(C_1) \neq 0)$.

Another classical rule consists in considering plausibility instead of belief. In the previous example, it would lead to:

- C_1 if $m(C_3) = 0$;
- C_3 if $m(C_1) = m(\{C_1, C_2\}) = 0$;
- $\{C_1, C_3\}$ if $m(C_3) \neq 0$ and $(m(C_1) \neq 0$ or $m(\{C_1, C_2\}) \neq 0)$.

These rules are somewhat different from the ones based on maximum belief. From a practical point of view, there are only very few situations where the decisions are actually different. Moreover, these rules involve $m(\{C_1, C_2\})$, which is less interesting here.

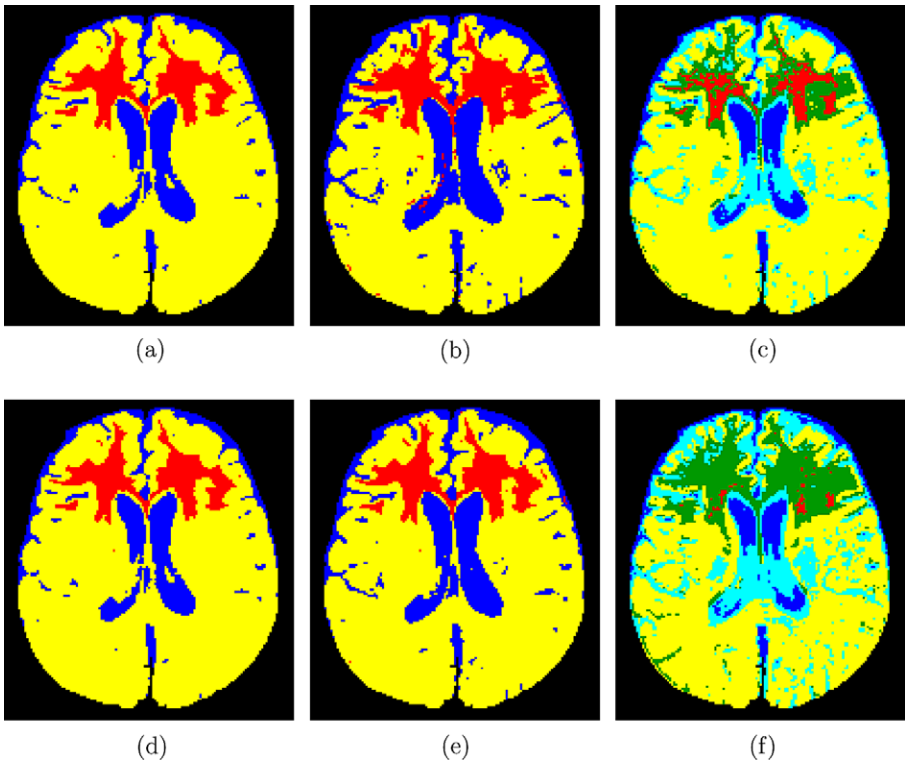

Fig. 26. Decision images based on the fusion of the masses obtained after morphological operations with different structuring elements. (a,d) Decision based on maximum of pignistic probability. (b,e) Decision based on maximum of belief over all singletons. (c,f) Decision based on maximum of belief over all subsets of D except D. (a–c) Smaller structuring element. (d–f) Larger structuring element.

A typical application of these results is to improve the computation of the volume of the pathology by taking into account not only the purely pathological tissues, but also the mixture areas. The decision for $\{C_1, C_3\}$ provides these areas, in which a further processing can lead to an estimation of the percentage of the pathological tissues. Such evaluations are much more robust to the positioning of the slices during the acquisition than evaluations based on crisp decisions.

The influence of the size of the structuring element is illustrated in Fig. 26, where the results can be compared to those in Fig. 25. It appears that the results are quite robust with respect to the choice of the structuring element. The decision based on pignistic probability remains the same. A few differences can be observed on the images showing the decision taken for maximum of belief over all subsets of D except D. Using a smaller structuring element, the intermediate area between pathology and normal brain is slightly smaller, while using a larger structuring element, it is larger. The main change is in the repartition between pure pathological class and the mixed class. Noticeably, the union of the mixed class and the pure pathological class (i.e. all pixels containing at least some pathological tissue) remains stable when changing the structuring element. This is an interesting result in terms of robustness of the proposed approach.

6. Conclusion

With the aim of fusing images under imprecision, we proposed in this paper a new method which introduces imprecision on the mass functions in the framework of belief functions, by using dual fuzzy morphological operators, such as erosion and dilation, or opening and closing. We have proved the consistency of the proposed approach, in terms of properties that have to be fulfilled by belief functions, in the case of crisp and fuzzy structuring elements. This method leads to an estimation of disjunctions of hypotheses that takes into

account the imprecision inherent to images and the considered classes or objects. The morphological operations can be applied either in the spatial domain, to represent spatial imprecision, or in a feature space (grey levels for instance), to represent the imprecision on the characteristics of the classes. Examples have been shown to illustrate both types of imprecision.

Acknowledgement

This paper is dedicated to the memory of Philippe Smets, with the warmest thanks for his encouraging support.

References

[1] I. Bloch (Ed.), Fusion d'informations en traitement du signal et des images, Hermès, Paris, France, 2003.
[2] P. Smets, The Combination of Evidence in the Transferable Belief Model, IEEE Transactions on Pattern Analysis and Machine Intelligence 12 (5) (1990) 447–458.
[3] G. Shafer, A Mathematical Theory of Evidence, Princeton University Press, 1976.
[4] T.D. Garvey, Evidential Reasoning for Land-Use Classification, in: Analytical Methods in Remote Sensing for Geographic Information Systems, International Association of Pattern Recognition, Technical Committee 7 Workshop, Paris, 1986.
[5] J.D. Lowrance, T.M. Strat, L.P. Wesley, T.D. Garvey, E.H. Ruspini, D.E. Wilkins, The Theory, Implementation and Practice of Evidential Reasoning, SRI Project 5701 final report, SRI, Palo Alto, June 1991.
[6] R.E. Neapolitan, A Survey of Uncertain and Approximate Inference, in: L. Zadeh, J. Kaprzyk (Eds.), Fuzzy Logic for the Management of Uncertainty, J. Wiley, New York, 1992, pp. 55–82.
[7] J.F. Baldwin, Inference for information systems containing probabilistic and fuzzy uncertainties, in: L. Zadeh, J. Kacprzyk (Eds.), Fuzzy Logic and the Management of Uncertainty, J. Wiley, New York, 1992, pp. 353–375.
[8] J. Gordon, E.H. Shortliffe, A method for managing evidential reasoning in a hierarchical hypothesis space, Artificial Intelligence 26 (1985) 323–357.
[9] S.Y. Chen, W.C. Lin, C.T. Chen, Evidential reasoning based on Dempster–Shafer theory and its application to medical image analysis, in: SPIE, vol. 2032, 1993, pp. 35–46.
[10] J. van Cleynenbreugel, S.A. Osinga, F. Fierens, P. Suetens, A. Oosterlinck, Road extraction from multi-temporal satellite images by an evidential reasoning approach, Pattern Recognition Letters 12 (1991) 371–380.
[11] P. Cucka, A. Rosenfeld, Evidence-based pattern matching relaxation, Technical Report CAR-TR-623, Center of Automation Research, University of Maryland, May 1992.
[12] K.M. Andress, A.C. Kak, Evidence accumulation and flow control in a hierarchical spatial reasoning system, AI Magazine (1988) 75–94.
[13] T. Lee, J.A. Richards, P.H. Swain, Probabilistic and evidential approaches for multisource data analysis, IEEE Transactions on Geoscience and Remote Sensing GE-25 (3) (1987) 283–293.
[14] H. Rasoulian, W.E. Thompson, L.F. Kazda, R. Parra-Loera, Application of the mathematical theory of evidence to the image cueing and image segmentation problem, in: SPIE Signal and Image Processing Systems Performance Evaluation, vol. 1310, 1990, pp. 199–206.
[15] E. Zahzah, Contribution à la représentation des connaissances et à leur utilisation pour l'interprétation automatique des images satellites, Thèse de doctorat, Université Paul Sabatier, Toulouse, 1992.
[16] T. Denœux, Construction belief functions from sample data using multimodal confidence regions, International Journal of Approximate Reasoning 42 (2006) 228–252.
[17] A. Appriou, Formulation et traitement de l'incertain en analyse multi-senseurs, in: Quatorzième Colloque GRETSI, Juan les Pins, 1993, pp. 951–954.
[18] A. Dromigny-Badin, S. Rossato, Y.M. Zhu, Fusion de données radioscopiques et ultrasonores via la théorie de l'évidence, Traitement du Signal 14 (5) (1997) 147–160.
[19] T. Denœux, A *k*-nearest neighbor classification rule based on Dempster–Shafer theory, IEEE Transactions on Systems, Man and Cybernetics 25 (5) (1995) 804–813.
[20] I. Bloch, Some aspects of Dempster–Shafer evidence theory for classification of multi-modality medical images taking partial volume effect into account, Pattern Recognition Letters 17 (8) (1996) 905–919.
[21] N. Milisavljevic, I. Bloch, Sensor fusion in anti-personnel mine detection using a two-level belief function model, IEEE Transactions on Systems, Man and Cybernetics 33 (2) (2003) 269–283.
[22] F. Tupin, I. Bloch, H. Maître, A first step towards automatic interpretation of SAR images using evidential fusion of several structure detectors, IEEE Transactions on Geoscience and Remote Sensing 37 (3) (1999) 1327–1343.
[23] I. Bloch, L. Aurdal, D. Bijno, J. Müller, Estimation of class membership functions for grey-level based image fusion, in: ICIP'97, Santa Barbara, CA, vol. III, 1997, pp. 268–271.
[24] D. Mercier, G. Cron, T. Denoeux, M. Masson, Fusion of multi-level decision systems using the transferable belief model, in: 8th International Conference on Information Fusion, FUSION'2005, Philadelphia, USA, 2005, pp. 655–658.

[25] S. Mascle, I. Bloch, D. Vidal-Madjar, Application of Dempster–Shafer evidence theory to unsupervised classification in multisource remote sensing, IEEE Transactions on Geoscience and Remote Sensing 35 (4) (1997) 1018–1031.
[26] M. Ménard, E.H. Zahzah, A. Shahin, Mass function assessment: case of multiple hypotheses for the evidential approach, in: Europto Conf. on Image and Signal Processing for Remote Sensing, Taormina, Italy, 1996.
[27] M. Rombaut, Fusion de données images segmentées à l'aide du formalisme de Dempster–Shafer, in: GRETSI'99, Vannes, France, 1999, pp. 655–658.
[28] P. Dokládal, Grey-scale image segmentation: a topological approach, Ph.D. thesis, Université Marne la Vallée, January, 2000.
[29] D. Dubois, H. Prade, R. Yager, Merging Fuzzy Information, in: J. Bezdek, D. Dubois, H. Prade (Eds.), Handbook of Fuzzy Sets Series, Approximate Reasoning and Information Systems, Kluwer, 1999 (Chapter 6).
[30] I. Bloch, H. Maître, Fuzzy mathematical morphologies: a comparative study, Pattern Recognition 28 (9) (1995) 1341–1387.
[31] I. Bloch, Using fuzzy mathematical morphology in the Dempster–Shafer framework for image fusion under imprecision, in: IFSA'97, Prague, 1997, pp. 209–214.
[32] A. Bendjebbour, Y. Delignon, L. Fouque, V. Samson, W. Pieczynski, Multisensor image segmentation using Dempster–Shafer fusion in Markov fields context, IEEE Transactions on Geoscience and Remote Sensing 39 (8) (2001) 1789–1798.
[33] W. Pieczynski, Multisensor triplet Markov chains and theory of evidence, International Journal of Approximate Reasoning 45 (1) (2007) 1–16.
[34] J. Serra, Image Analysis and Mathematical Morphology, Academic Press, London, 1982.
[35] H.J.A.M. Heijmans, C. Ronse, The algebraic basis of mathematical morphology – Part I: Dilations and erosions, Computer Vision, Graphics and Image Processing 50 (1990) 245–295.
[36] C. Ronse, H.J.A.M. Heijmans, The algebraic basis of mathematical morphology – Part II: Openings and closings, Computer Vision, Graphics and Image Processing 54 (1991) 74–97.
[37] H.J.A.M. Heijmans, Morphological Image Operators, Academic Press, Boston, 1994.
[38] P. Smets, The normative representation of quantified beliefs by belief functions, Artificial Intelligence 92 (1997) 229–242.
[39] G.J. Klir, T.A. Folger, Fuzzy Sets, Uncertainty, and Information, Englewood Cliffs, 1988.
[40] D. Dubois, H. Prade, Representation and combination of uncertainty with belief functions and possibility measures, Computational Intelligence 4 (1988) 244–264.
[41] D. Dubois, H. Prade, Fuzzy sets and probability: misunderstandings, bridges and gaps, in: 2nd IEEE Int. Conf. on Fuzzy Systems, 1993, pp. 1059–1068.
[42] G.J. Klir, Principles of uncertainty: what are they? why do we need them? Fuzzy Sets and Systems 74 (1995) 15–31.
[43] B. de Baets, Idempotent closing and opening operations in fuzzy mathematical morphology, in: ISUMA-NAFIPS'95, College Park, MD, 1995, pp. 228–233.
[44] D. Sinha, E.R. Dougherty, Fuzzification of set inclusion: theory and applications, Fuzzy Sets and Systems 55 (1993) 15–42.
[45] V. di Gesu, M.C. Maccarone, M. Tripiciano, Mathematical morphology based on fuzzy operators, in: R. Lowen, M. Roubens (Eds.), Fuzzy Logic, Kluwer Academic, 1993, pp. 477–486.
[46] B. de Baets, Fuzzy morphology: a logical approach, in: B. Ayyub, M. Gupta (Eds.), Uncertainty in Engineering and Sciences: Fuzzy Logic, Statistics and Neural Network Approach, Kluwer Academic, 1997, pp. 53–67.
[47] M. Nachtegael, E.E. Kerre, Classical and fuzzy approaches towards mathematical morphology, in: E.E. Kerre, M. Nachtegael (Eds.), Fuzzy Techniques in Image Processing, Studies in Fuzziness and Soft Computing, Physica-Verlag, Springer, 2000, pp. 3–57 (Chapter 1).
[48] T.-Q. Deng, H. Heijmans, Grey-Scale Morphology Based on Fuzzy Logic, Journal of Mathematical Imaging and Vision 16 (2002) 155–171.
[49] I. Bloch, Duality vs adjunction and general form for fuzzy mathematical morphology, in: WILF, Crema, Italy, LNCS, vol. 3849, 2005, pp. 354–361.
[50] I. Bloch, C. Pellot, F. Sureda, A. Herment, Fuzzy modelling and fuzzy mathematical morphology applied to 3D reconstruction of blood vessels by multi-modality data fusion, in: D.D.R. Yager, H. Prade (Eds.), Fuzzy Set Methods in Information Engineering: A Guided Tour of Applications, John Wiley & Sons, New-York, 1996, pp. 93–110 (Chapter 5).
[51] J.A. Barnett, Computational methods for a mathematical theory of evidence, in: Proc. of 7th IJCAI, Vancouver, 1981, pp. 868–875.
[52] P. Smets, Constructing the Pignistic probability function in a context of uncertainty, Uncertainty in Artificial Intelligence 5 (1990) 29–39.